Polymer Journal (2024) 56:791–818
https://doi.org/10.1038/s41428-024-00920-x

REVIEW

Recent advances in structurally elaborate triptycenes, triptycene-containing polymers and assemblies: structures, functions and applications

Fumitaka Ishiwari[1,2,4] · Yoshiaki Shoji[1,2,3] · Colin J. Martin[1] · Takanori Fukushima[1,2,3]

Received: 29 March 2024 / Revised: 24 April 2024 / Accepted: 29 April 2024 / Published online: 29 May 2024

Abstract

Triptycene, a rigid propeller-shaped molecule, was first synthesized in the early 1940s. More recently, many triptycene-containing polymers and molecular assemblies have been developed for a wide range of applications, including guest recognition, material transport, separation, catalysis, and as device components. The advantages of triptycenes lie in their ability to introduce a variety of functional groups on their three-dimensional backbone, with changes in substitution patterns as well as the type of substituents present having a significant impact on the material properties. In this review, we describe the synthesis of triptycene derivatives and polymers, detailing selected examples of triptycene-containing functional polymers. We also focus on the construction of triptycene-based two-dimensional assemblies and polymers, where space-filling designs based on rigid propeller-shaped skeletons are essential. Through a thorough literature survey, future directions and possibilities for the development of triptycene-containing functional materials are discussed.

Introduction

Triptycene is a rigid molecule with a three-dimensional (3D) skeleton consisting of three phenylene rings arranged with interblade angles of 120° (Fig. 1a) [1–10]. Triptycene derivatives have been utilized in many fields, including supramolecular chemistry and polymer and materials science, and researchers have taken advantage of the structural features of triptycenes in the development of functional molecules, polymers, and assemblies. For example, a number of triptycene-containing polymers (trip-polymers) have been reported [2, 10], many of which exhibit microporosity, can serve as low dielectric materials, and show specific assembly properties arising from the large free volumes present around the rigid triptycene skeleton. Importantly, the properties of trip-polymers largely depend on their substitution patterns, the symmetry of the constituent triptycene units, and the type of substituents present. To date, synthetic methods for accessing triptycene derivatives have been intensely developed, allowing the introduction of various substituents at different positions (Fig. 1b). These structurally elaborate triptycene derivatives are useful for the design of various functional polymers (Fig. 1c–f). Our group has also been engaged in the development of trip-polymers that exhibit unique assembly properties, for which triptycene units with particular substitution patterns [11], different from the majority of previously reported trip-polymers, are essential (*vide infra*).

In this review, based on a thorough literature survey, we describe the synthesis and structures of triptycene derivatives and trip-polymers with various substitution patterns while summarizing recent research trends. To the best of our ability, we attempted to avoid including examples of trip-polymers that have already been described in the book and review by C-F. Chen et al. [1, 8]. We also describe the formation of two-dimensional (2D) assemblies and related polymers using

✉ Takanori Fukushima
fukushima@res.titech.ac.jp

[1] Laboratory for Chemistry and Life Science, Institute of Innovative Research, Tokyo Institute of Technology, 4259 Nagatsuta, Midori-ku, Yokohama 226-8501, Japan

[2] Department of Chemical Science and Engineering, School of Materials and Chemical Technology, Tokyo Institute of Technology, 4259 Nagatsuta, Midori-ku, Yokohama 226-8501, Japan

[3] Research Center for Autonomous Systems Materialogy (ASMat), Institute of Innovative Research, Tokyo Institute of Technology, 4259 Nagatsuta, Midori-ku, Yokohama 226-8501, Japan

[4] Present address: Department of Applied Chemistry, Graduate School of Engineering, Osaka University, 2-1 Yamadaoka, Suita, Osaka 565-0871, Japan

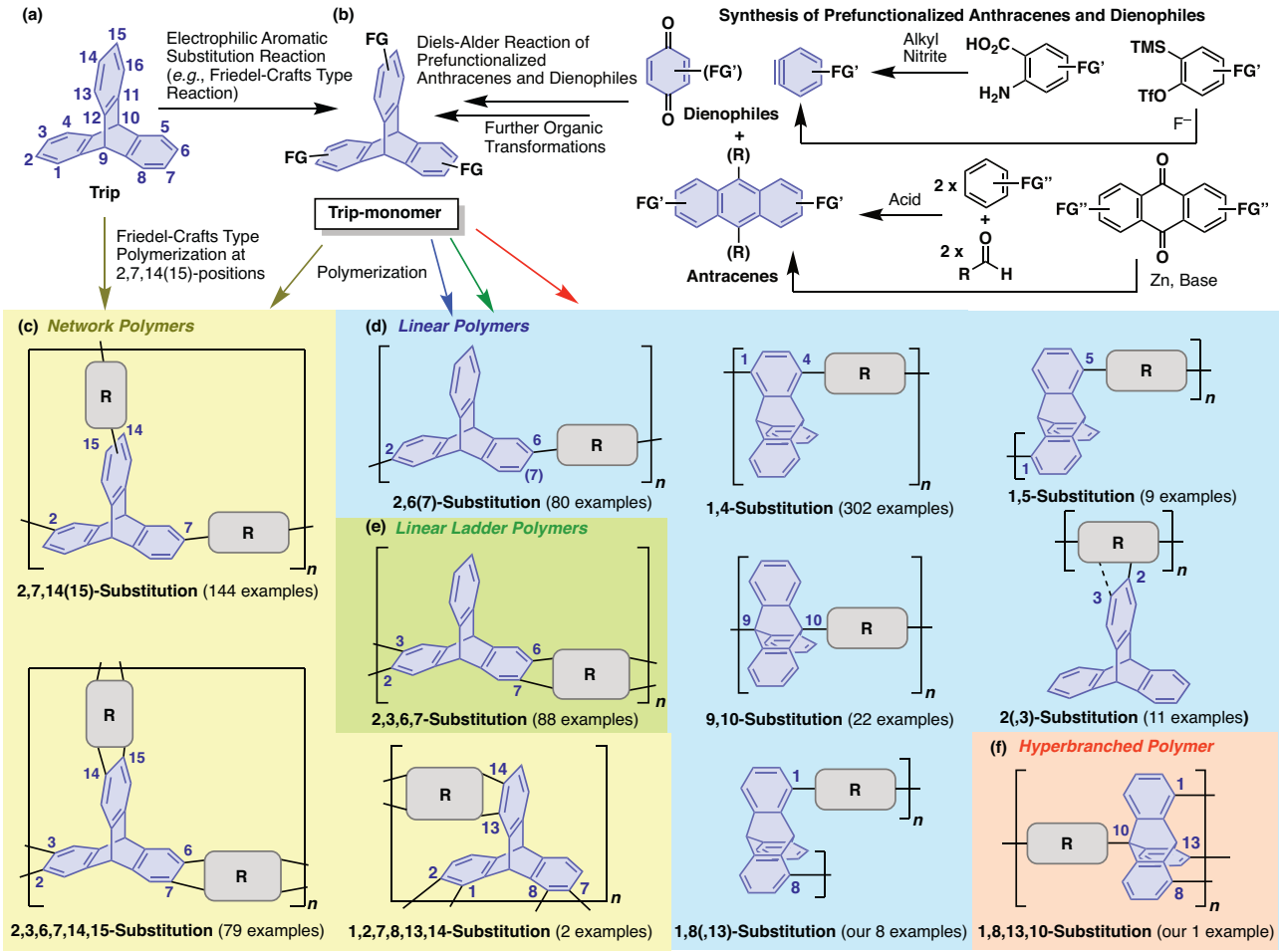

Fig. 1 **a** Molecular structure of triptycene with carbon numbering. **b** Synthesis and (**c**–**f**) schematic drawings of trip-polymers with (**c**) network, (**d**) linear, (**e**) linear ladder, and (**f**) hyperbranched structures

particular types of triptycenes. Triptycene derivatives, when appropriately functionalized, self-assemble into either porous or dense (nonporous) 2D structures through intermolecular π-stacking and/or nested packing of their propeller-blade moieties. These triptycene-based 2D assemblies are useful for the construction of polymeric materials featuring long-range structural order. We also describe various applications of triptycene-based 2D assemblies, including the development of polymer materials with enhanced properties for high-performance organic electronic devices.

Literature survey

Our manual survey of academic papers (other than patents) using Google Scholar® in March 2024 with the keywords "triptycene + polymer" and "iptycene + polymer" revealed that 364 research publications reported a total of 923 triptycene- and iptycene-containing polymers from 1968 to the present. Note that (i) when polymers with the same structure were reported in different publications, we included them multiple times in the count, (ii) copolymers were counted separately, and (iii) metal-organic frameworks were excluded. Figure 2 shows histograms of the numbers of published papers (Fig. 2a) and trip-polymers (Fig. 2b) reported in these papers, where the colors in Fig. 2b corresponds to the substitution patterns of the constituent triptycene units. Figure 2c shows the percentage of polymers with each substitution pattern of triptycene relative to all trip-polymers; linear polymers linked at the 1,4-positions (338 examples) are the most common, followed by network polymers linked at the 2,7,14(15)-positions (189 examples), linear ladder polymers linked at the 2,3,6,7-positions (118 examples), linear polymers linked at the 2,6(7)-positions (92 examples) and network polymers linked at the 2,3,6,7,14,15-positions, including 2D/3D covalent organic frameworks (COFs) (107 examples) [12]. These polymers account for *ca*. 90% of the total number of trip-polymers. Both the reported number of papers and the number of trip-polymers rapidly increased around 2010. In the following, we describe the research trends related to triptycene-based polymers and assemblies in chronological order.

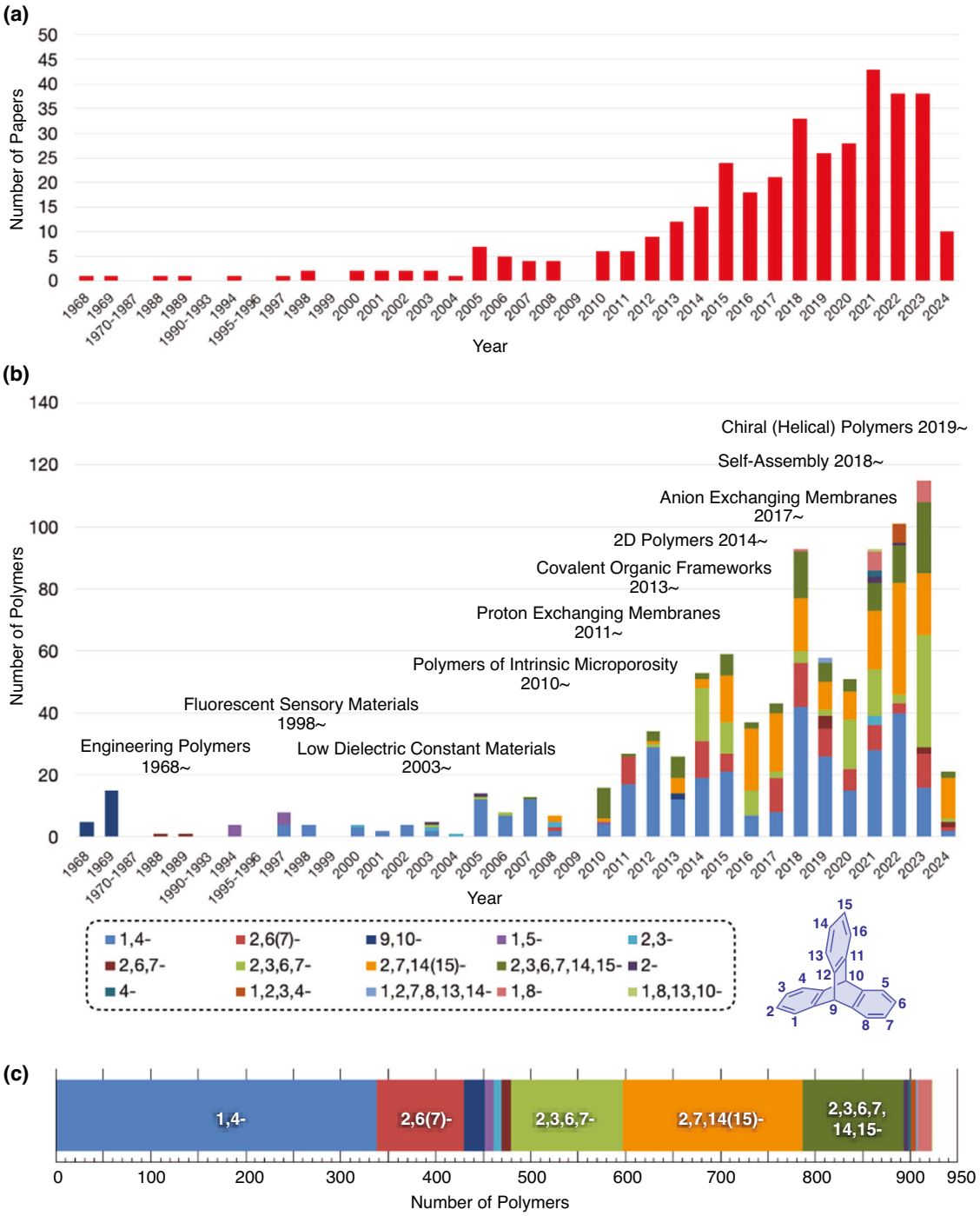

Fig. 2 **a** Histogram of the number of annual publications on trip-polymers. **b** Histogram and distribution of the number and substitution patterns of trip-polymers reported per year. **c** Summary of the distribution of substitution patterns in reported trip-polymers

Early-stage examples including engineering polymers, fluorescent sensors, and low-dielectric materials

The first trip-polymer was reported in 1968 [13]. In that period, colorless, heat-resistant engineering plastics were the focus of attention, and structurally rigid triptycene derivatives with a small π-conjugated system were predicted to be potent building blocks in this area [14]. In 1998, Swager et al. reported a seminal paper describing the detection of explosives (TNT; trinitrotoluene) using π-conjugated polymers containing pentiptycene in the main chain [15]. Since then, a series of related papers have been published. Swager et al. also developed low-*k* polymers that

serve as insulating interlayer materials for high-density electronic devices [16]. Trip-polymers with large free volumes around their polymer backbones tend to have low relative permittivity.

PIMs, COFs and 2D polymers (2000s~)

In 2004, McKeown et al. reported ladder polymers with rigid and contorted main chains that yielded microporous freestanding membranes featuring very high specific surface areas [17] and named them "polymers of intrinsic microporosity (PIMs)" [9, 18, 19]. Since then, PIMs have been studied extensively as membranes for gas separation and storage. Structurally rigid triptycenes, to which a variety of substituents can be introduced, are excellent building blocks for PIMs. Yaghi et al. and others introduced the concept of covalent organic frameworks (COFs) using similar porous solid materials in 2005 [12, 20]. Propeller-shaped triptycenes also serve as useful building blocks for 2D and 3D COFs, and an increasing number of triptycene-based COFs have been reported since 2013. The synthesis of exfoliable triptycene-based 2D polymers with single-crystal-like structural order has been achieved using triptycene derivatives consisting of extended propeller blades [21, 22].

Ion-conducting membranes (2010s~)

In 2011, a trip-polymer that serves as an excellent proton exchange membrane for fuel cells was first reported [23]. Then, triptycene-based anion exchange membranes for use as alkaline fuel cells were reported in 2017 [24]. While the initial focus in the development of these ion-exchange membranes was on introducing dense ionic functional groups on the triptycene moieties, later works shifted toward designs that take advantage of the microporous nature of trip-polymers.

Self-assembled materials (2010s~)

The abovementioned examples of trip-polymers all exhibit porosity and utilize micro- and nanopores, e.g., material transport and separation. In 2015, our research group reported that triptycene derivatives with alkoxy groups at the 1,8,13-positions self-assemble to fill the free volume between neighboring triptycene molecules, forming a 2D nested hexagonal packing arrangement, which has been applied in the development of polymers with new functionalities [11].

Chiral polymers (2010s~)

Triptycenes substituted at two or more positions, such as 2,6- or 1,5-substituted derivatives, are inherently chiral [7]. However, until recently, such chiral triptycenes have not been actively explored. Recently, chiral polymers utilizing this triptycene chirality have been reported, and their functions have attracted increased amounts of attention.

In the following sections, we will discuss general synthetic methods for trip-polymers, and their structures and applications. This review builds upon the examples found in the 2013 book of C-F. Chen et al., in which they describe a chapter on trip-polymers [1]. As such, we will focus on results published after this date.

Synthetic routes for accessing triptycene derivatives and triptycene-containing polymers

As shown in Fig. 1b, there are two major ways to synthesize trip-polymers: direct polymerization of unsubstituted triptycene or polymerization using a triptycene monomer (trip-monomer) substituted with a reactive functional group. Unsubstituted triptycene (**1**) easily reacts at its 2,7,14(,15)-positions under Friedel-Crafts-type conditions. Although monomer (**1**) can be easily prepared, this polymerization method does not yield network polymers containing triptycenes linked at the 2,7,14(,15)-positions. Trip-polymers linked at other substitution positions require the synthesis of trip-monomers, in which reactive substituents are introduced at the desired positions in advance. One method is to introduce substituents at the 2(,3)(,6),7,14(,15)-positions by Friedel–Crafts-type reactions with **1**. The main trip-monomers synthesized starting with this method are shown in Fig. 3. The Friedel–Crafts conditions used include nitration with nitric acid [25, 26], acylation using Lewis acid catalysts such as aluminum chloride or tin chloride, and formylation [27]. For nitration, 2-monosubstituted (**2**), 2,6- (**3**) or 2,7-disubstituted (**4**) and 2,6,14- (**5**) or 2,7,14-trisubstituted (**6**) nitro triptycene derivatives have been reported. The ratios of formation can be controlled somewhat selectively by varying the amounts of reagents used, and importantly, all isomers can be separated using silica gel column chromatography (except for optical isomers). This has allowed for the synthesis of trip-monomers with the desired number and patterns of nitro substituents. Amino-substituted triptycenes (**7**–**11**), obtained by reducing nitro moieties, are frequently used as monomers in the synthesis of polyamides, polyimides, and Tröger's base-containing PIMs [9, 19]. Sandmeyer-type reactions *via* diazotization of the amino forms have led to the insertion of halo substituents, yielding bromo (**12**–**16**) and iodo (**17**–**21**) triptycenes [26, 28] along with an azide-substituted trip-monomer (**22**) [29, 30], which have been used in various transition-metal-catalyzed couplings and click polymerizations. In addition, 2,6-diaminotriptycene (**8**) [31] and its

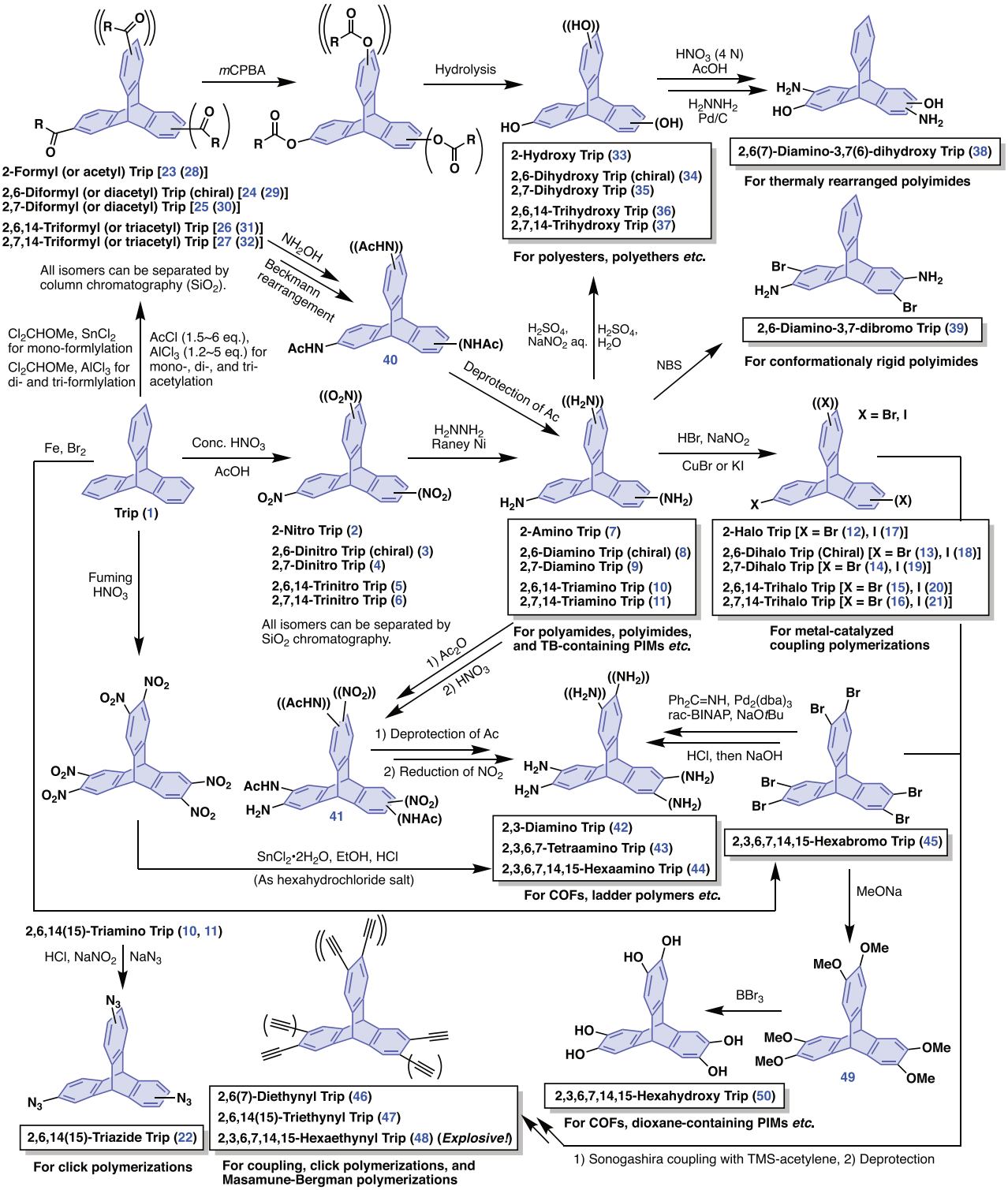

Fig. 3 Synthesis of trip-monomers from unsubstituted triptycene **1**

derivatives [32] are relatively easy to separate optically using chiral HPLC, and chiral polymers with interesting optically active functions have been obtained, which will be described in detail later. Although most of the trip-monomers shown here are chiral, many optically active monomers and polymers are expected to be developed in the future.

Baeyer–Villiger oxidation of acylated trip-monomers (**23**–**32**) with *m*CPBA and subsequent hydrolysis have led to hydroxy trip-monomers for use in polyester and

polyether synthesis (**33**–**37**) [27, 33]. These compounds have also been synthesized by other methods [34] and will be described later. Nitration and reduction of 2,6(,7)-dihydroxytriptycene (**34,35**) yields a trip-monomer with two hydroxy and two amino groups (**38**) [33]. This type of monomer is important in the preparation of polybenzimidazoles [35] through thermal rearrangement to the corresponding hydroxy group-containing polyimides, which have been shown to act as excellent gas-separation membranes [36]. Another monomer related to gas separation membranes, the di-*ortho*-brominated 2,6(,7)-diaminomonomer (**39**), which is useful in the synthesis of polyimides with reduced free rotation, has recently been reported [37, 38]. A route to synthesize triaminotriptycenes via Beckmann-rearrangement (**40**) from acetylated triptycenes (**23**–**32**) is also known [27].

Amino- and/or bromo-substituted monomers can be synthesized by reacting with unsubstituted triptycene **1** to yield, for example, 2,3,6,7,14,15-hexasubstituted trip-monomers. For the di-amination (**42**), tetra-amination (**43**) and hexa-amination (**44**) of triptycenes, a multistep synthesis *via* protection, nitration (**41**), deprotection, and reduction of triaminotriptycene (**10,11**) was originally reported [39]. Later, Mastalerz et al. reported that amino-substituted derivatives can be synthesized as the corresponding hydrochloride salts in two steps from **1** using fuming nitric acid [40]; however, the yield from **1** is only 18%. On the other hand, for the synthesis of hexabromotriptycene (**45**), bromination of **1** using Br_2 in the presence of iron proceeded in relatively high yield [41]. Very recently, the addition of I_2 was shown to increase the yield to 90% [42]. It has been reported that hexaaminotriptycene (**44**) can be synthesized efficiently by palladium-catalyzed Buchwald–Hartwig amination of hexabromide with benzophenone imine, followed by deprotection with hydrochloric acid [43]. This hexa-aminated trip-monomer is widely used as a building block for COFs and network polymers. Sonogashira couplings with di-, tri-, and hexa-brominated monomers have led to ethynyl-substituted trip-monomers (**46**–**48**) that can be used in further Sonogashira couplings and click polymerizations. 2,3,6,7,14,15-Hexaethynyltriptycene (**48**) can be used for Masamune–Bergman polymerizations, resulting in interesting porous network polymers [44, 45], which will be discussed in detail later. Hexa-hydroxylated trip-monomers (**50**) can also be synthesized by treating the hexa-brominated trip-monomers with sodium methoxide to introduce methoxy groups (**49**) and then removing the methyl group using BBr_3 [46]. This approach has been used in the preparation of COFs and PIMs. In addition to the synthetic methods described thus far, it is also possible to prepare amino substituents from acyl groups by Beckmann rearrangement and hydrolysis [27] and hydroxyl substituents from amino groups by Sandmeyer-type reactions [25], but as of yet, no polymers have been obtained using monomers in these ways. Moreover, direct borylation of **1** using an iridium catalyst and bis(pinacolato)diboron has been reported to yield 2,6,14(15)-tris[(pinacolato)boryl]triptycene as a mixture of regioisomers [47]. The propeller blades of these triboryltriptycenes can be extended using Suzuki coupling and dehydrogenative cyclization. Thus, triboryltriptycenes could be useful as building blocks for network polymers.

Another method to synthesize trip-monomers is to introduce functional groups into anthracenes, benzynes, or quinones, which are common precursors in the synthesis of triptycenes. In addition to simple modification reactions, anthracene derivatives with various functional groups can be derived from commercially available anthraquinone. Anthracenes can also be synthesized using aromatic electrophilic substitution reactions between relatively electron-rich benzenes and reagents such as aldehydes or dichloromethane. A number of commercially available substituted benzyne precursors, including anthranilic acids and derivatives with triflate and trimethylsilyl groups, have been used.

The synthesis of the most common 1,4-substituted triptycene derivatives is shown in Fig. 4. *para*-Benzoquinone (**51**) has been used as a dienophile with anthracenes (**52, 53**) in Diels-Alder reactions, followed by aromatization to the 1,4-dihydroxy trip-monomer (**54, 55**) [16, 17]. From this, a perfluorosulfonated intermediate (**56**) can be formed and converted into a 1,4-diethynyl trip-monomer (**57**) by Sonogashira coupling [48]. From the 1,4-dihydroxy trip-monomer (**54**), a *para*-benzoquinone derivative (**59**) can be obtained by oxidation, and from the imine derivative (**60**), it can be prepared through condensation with hydroxylamine, which can be subsequently reduced to yield the 1,4-diamino trip-monomer (**61**) [49, 50]. Compound **61** can undergo a Sandmeyer-type reaction to yield the 1,4-diiodo trip-monomer (**62**) [48], which has been used in a further Sonogashira reaction to synthesize the 1,4-diethynyl trip-monomer (**57**) [51, 52]. The *para*-benzoquinone form of pentiptycene (**64**) can be synthesized using an excessive amount of anthracene in a Diels–Alder reaction with *para*-benzoquinone or by allowing the *para*-benzoquinone form of triptycene to undergo a second Diels–Alder reaction with anthracene in acetic acid [16, 48]. A reduction of **64** yields the 1,4-dihydroxypentiptycene monomer (**63**) [52], whereas a nucleophilic attack of **64** with a TMS-acetylide (**65**) and subsequent oxidation (**66**) and deprotection yields the 1,4-diethynylpentiptycene monomer (**58**) [16, 48]. However, it has been noted that the equivalent 1,4-diaminopentiptycene cannot be synthesized by a similar route [4, 48, 53].

It has been reported that functionalized triptycenes and pentiptycenes can be obtained by reacting substituted anthracenes with benzoquinone **51**. The reaction of

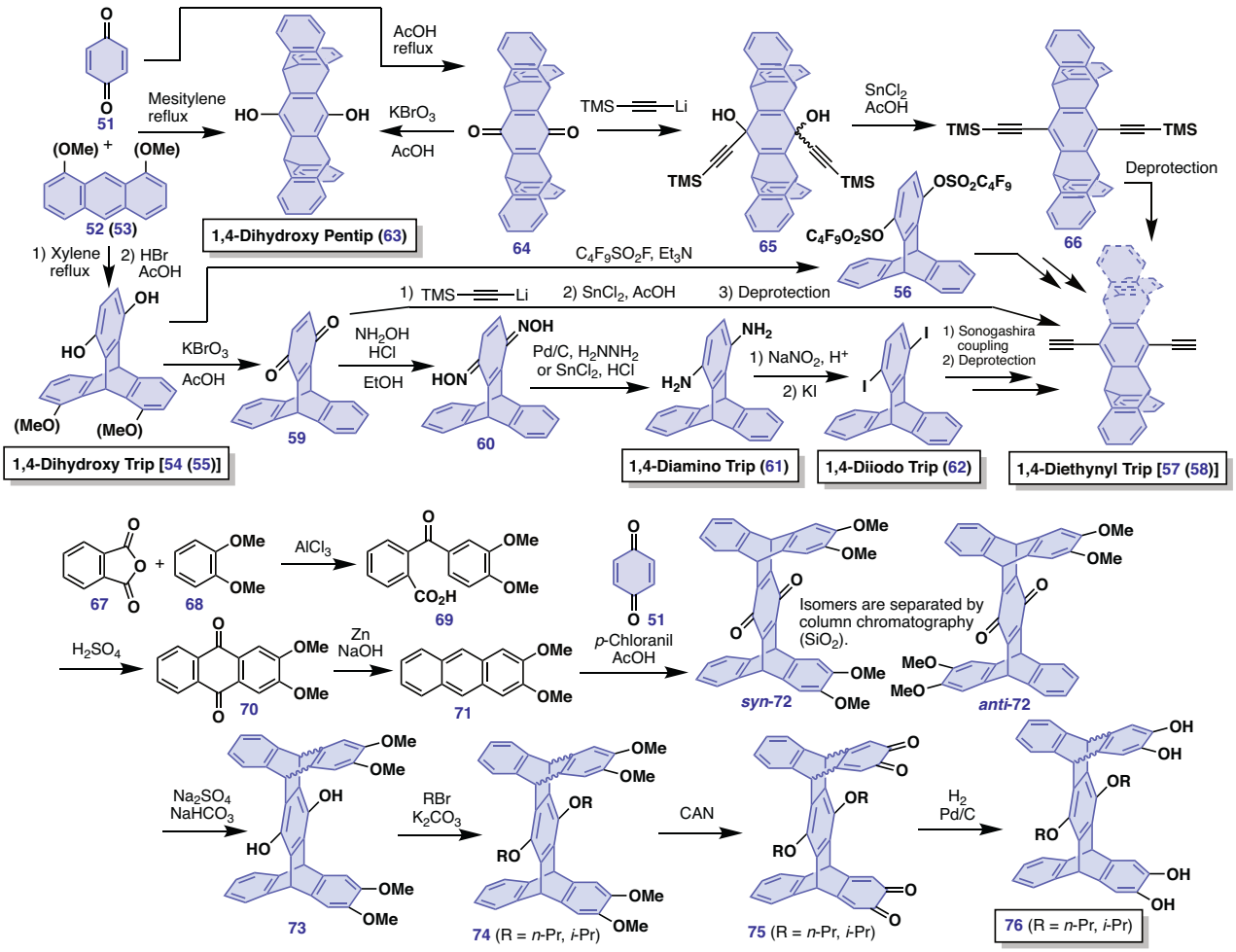

Fig. 4 Synthesis of 1,4-substituted trip-monomers

1,8-dimethoxyanthracene (**53**) with **51** yields 1,4-dihydroxytriptycene (**55**), which has two hydroxy substituents protected by methyl groups [54]. In 2021, a highly functionalized pentiptycene monomer was synthesized by Guo et al. [55]. They synthesized 2,3-dimethoxyanthracene (**71**) from phthalic anhydride (**67**) and dimethoxybenzene (**68**) by stepwise Friedel–Crafts reactions (**69**) and subsequent reduction/aromatization (**70,71**). The reaction of **71** with *para*-benzoquinone **51** gave a pentiptycene (**72**) bearing upper and lower methoxy groups as a mixture of *syn*- and *anti*-isomers. These isomers can be separated by means of silica gel column chromatography. The central *para*-benzoquinone moiety of **72** can be reduced (**73**) and etherified (**74**). The use of ceric ammonium nitrate (CAN) for the reaction with **74** resulted in the selective oxidation of the dimethoxybenzene moieties to yield the *ortho*-quinone pentiptycene (**75**). This was reduced *via* a hydrogenation reaction to yield a tetrahydroxy derivative (**76**) [55], which has been used in the preparation of PIMs [9].

Figure 5 shows the synthetic pathway for accessing triptycenes with hydroxyl, carboxyl, carboxylic acid chloride, isocyanate, and amino groups as polymerizable substituents at the 9,10-positions. The 9,10-positions of unsubstituted anthracene (**77**) were chloromethylated (**78**) and converted to acetoxy groups *via* nucleophilic substitution (**79**), followed by a Diels–Alder reaction with benzyne generated from anthranilic acid (**80**) and amyl nitrite to yield 9,10-diacetoxymethyltriptycene (**81**). The acetyl group can then be deprotected to the 9,10-dihydroxymethyl trip-monomer (**82**) [14, 15]. It is also possible to synthesize a 9,10-dihydroxyethyl trip-monomer (**86**) through the introduction of a cyano group (**83**) via nucleophilic substitution of the chloromethyl group of **78** and subsequent functional group transformation followed by a Diels–Alder reaction (**84, 85**) [15]. Oxidation of the 9,10-dihydroxymethyl trip-monomer (**82**) with chromium trioxide yields the 9,10-dicarboxyl trip-monomer (**87**), and further treatment with thionyl chloride yields the 9,10-dichlorocarbonyl trip-monomer (**88**). This synthetic method, reported in 1968 and 1969 [13, 14], is still used today. For example, compound **87** has been utilized for the synthesis of MOFs [56]. 9,10-Diamino Trip-monomer (**91**) [14, 15] can be

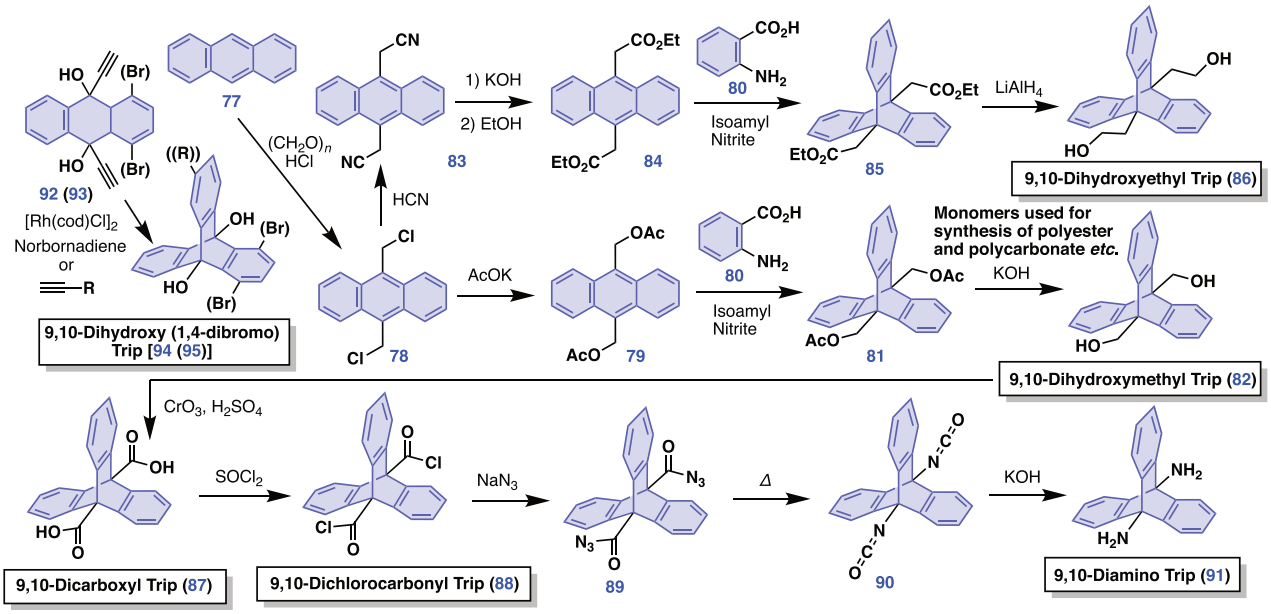

Fig. 5 Synthesis of 9,10-functionalized trip-monomers

synthesized from **88** through a reaction with sodium azide, a thermal Curtius rearrangement of the resulting benzoyl azide (**89**), and the subsequent hydrolysis of a diisocyanate derivative (**90**). 9,10-Functionalized triptycene derivatives such as **87** and **91** have been used as building blocks for polyesters and polyamides. Moreover, an interesting synthetic method has been developed for 9,10-dihydroxylated derivatives (**94, 95**). For example, anthracene substituted with hydroxyl and ethynyl groups at the 9- and 10-positions (**92**) reacts with norbornadienes or terminal alkynes in the presence of a rhodium catalyst in a [2+2+2] cycloaddition to form 9,10-dihydroxytriptycene **94** [57, 58]. Cycloaddition with terminal alkynes or norbornadienes affords derivatives with or without a substituent at the 14-position, respectively. This synthetic protocol can be applied to the synthesis of a highly substituted, 1,4-dibrominated derivative (**95**) from a corresponding precursor (**93**) [57]. Sonogashira coupling polymerization using **95** yields polyphenylene ethynylenes, which can be transformed to polyphenylene vinylenes through intramolecular hydrooxygenation of alkyne moieties.

Figure 6 summarizes the trip-monomers that can be synthesized from functionalized anthraquinones. The chloro groups of 1,5-dichloroanthraquinone (**96**) can be converted to cyano groups (**97**) using copper cyanide and then to carboxylic acids (**98**) by hydrolysis [59]. The anthraquinone skeleton is reduced to anthracene by treatment with zinc under basic conditions (**99**), which is followed by methylation of the carboxylic acid moieties to yield the methyl ester derivative (**100**). Subsequently, **100** reacts with benzyne generated from anthranilic acid (**80**) and isoamyl nitrite to yield a triptycene with ester groups at the 1,5-positions (**101**). Hydrolysis of **101** yields the 1,5-dicarboxytriptycene monomer (**102**). Here, the 1,5-diaminotriptycene monomer (**106**) can be synthesized through acid chloride (**103**), benzoyl azide (**104**), and isocyanate (**105**) intermediates, similar to the case of **91** in Fig. 5 [59]. 1,5-Dicarboxytriptycene (**102**) is chiral, and its enantiomeric separation has been achieved by the formation of diastereomeric salts with the naturally occurring optically active alkaloids synconidine or synconine. Thus, (*R,R*)- and (*S,S*)-1,5-dicarboxytriptycene have been obtained using synconidine and synconine, respectively [59]. The use of these 1,5-dicarboxytriptycenes results in the formation of the corresponding optically active 1,5-diamino trip-monomers (**106**), which can be further transformed into optically active 1,5-dihydroxy trip-monomers (**107**) by reaction with water *via* a diazonium salt [59].

The synthesis of 1,5-dihydroxy trip-monomer (**107**) has also been reported using the scheme shown in the lower part of Fig. 6 [60]. A sodium salt of anthracene-1,5-disulfonic acid (**109**), synthesized from the corresponding anthraquinone (**108**), is subjected to alkali fusion, affording 1,5-dihydoxytriptycene (**110**). After reacting with acetic anhydride, the resulting 1,5-diacetoxyanthracene (**111**) reacts with benzyne, followed by hydrolysis to yield the 1,5-dihydroxy trip-monomer (**107**) [60]. For 2,6-dihydroxytriptycene (**34**) [34], 2,6-dihydroxyanthraquinone (**113**) has been used as a starting material. Compound **113** is converted to 2,6-dimethoxyanthracene (**116**) *via* methylation and reduction (in no particular order) [61, 62], and then **116** reacts with benzyne followed by demethylation using boron tribromide to yield 2,6-dihydroxytriptycene **34**. Therefore, 1,5-dihydroxyanthraquinone (**117**) may provide an

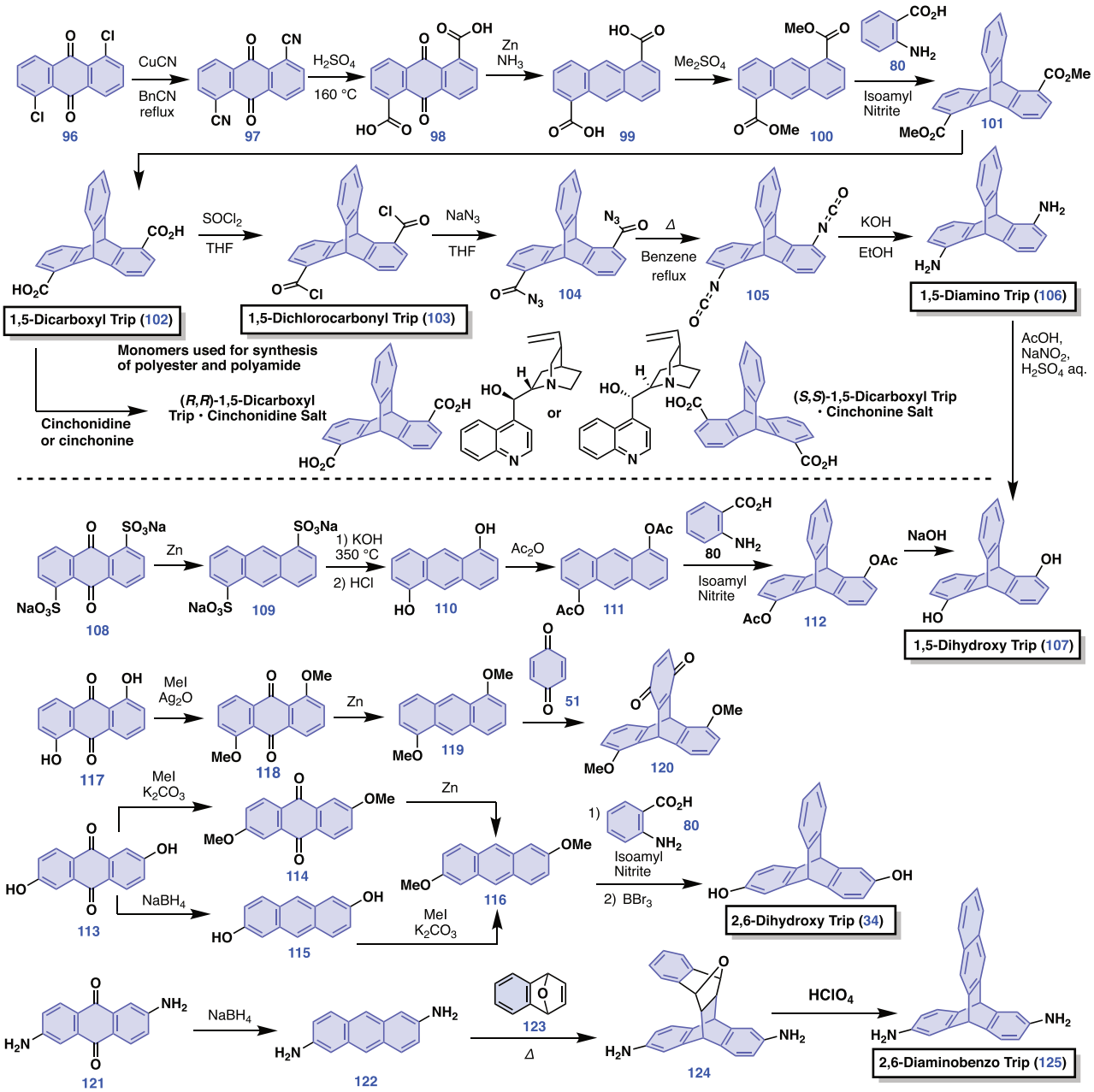

Fig. 6 Synthesis of trip-monomers from functionalized anthraquinones

alternative synthetic route to 1,5-dihydroxytriptycene **107**, which does not involve alkali fusion. It has been reported that 1,5-dimethoxyanthracene (**119**) derived from **117**, upon reaction with *para*-benzoquinone (**51**), yields 1,5-dimethoxytriptycene monobenzoquinone (**120**) [63]. *para*-Benzoquinone is useful in the synthesis of benzoquione derivatives of triptycene [64]. 2,6-Diaminoanthracene (**122**), obtained by the reduction of 2,6-diaminoanthraquinone (**121**) [65], has been reacted with 1,4-epoxy-1,4-dihydronaphthalene (**123**) under Diels–Alder conditions to form **124**, followed by dehydration using perchloric acid to yield 2,6-diaminobenzotriptycene (**125**) [66]. The Diels–Alder reaction using **123**, which can be carried out even in the presence of amino functionalities, is useful for the synthesis of benzotriptycene derivatives. Compound **125** has been used for the synthesis of microporous polyimides and PIMs consisting of Tröger's base moieties [66].

Figure 7 summarizes the synthesis of highly functionalized trip-monomers using multisubstituted anthracene derivatives. These triptycene derivatives have attracted much attention in recent years as monomers for use in the preparation of ladder polymer-based PIMs and microporous polyimides. The Friedel–Crafts reaction of 1,2-dimethoxybenzene (**68**) with various aldehydes (**126**) in the presence

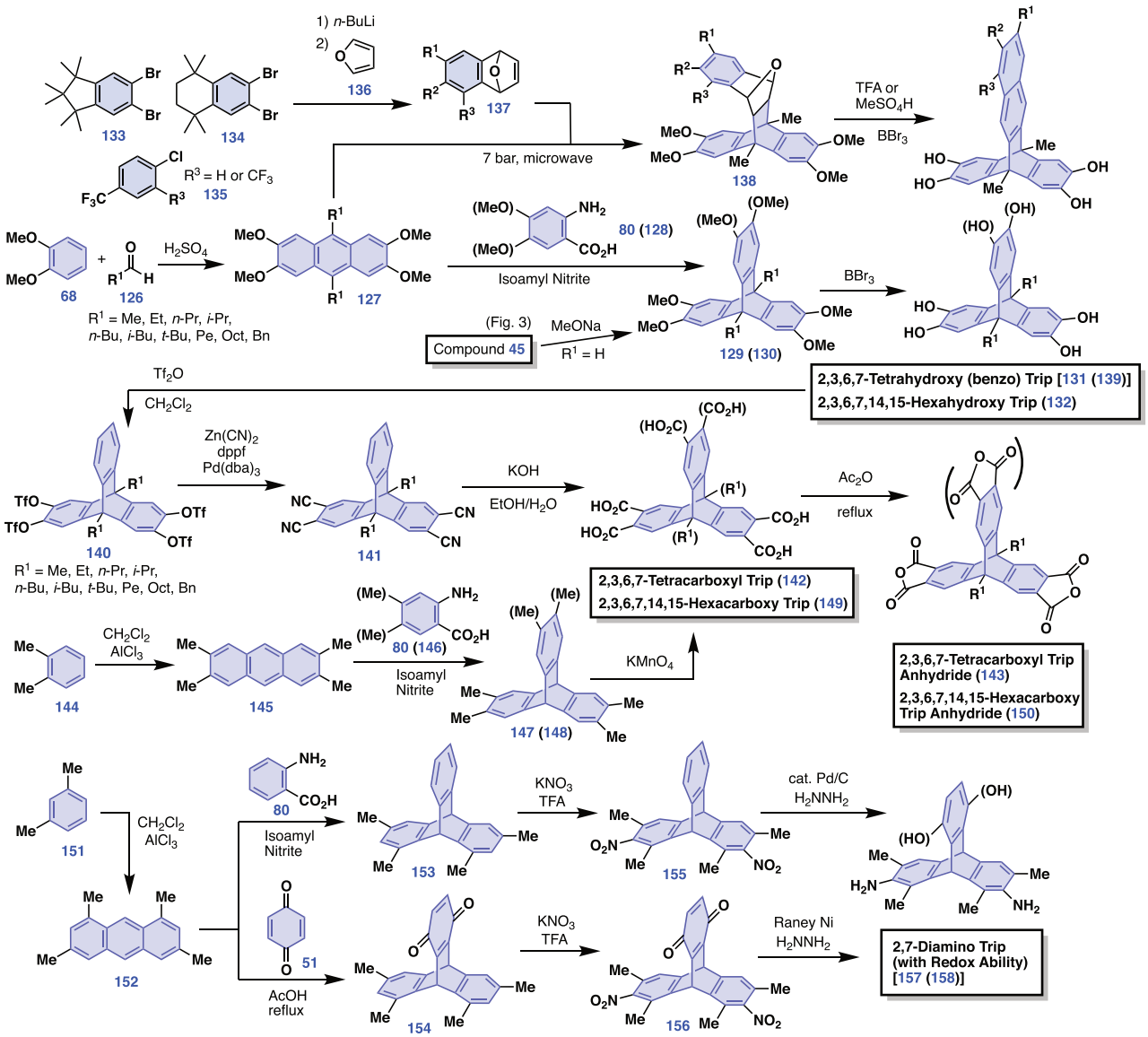

Fig. 7 Synthesis of trip-monomers from multifunctionalized anthracenes

of sulfuric acid yields the corresponding hexa-substituted 9,10-dialkyl-2,3,6,7-tetramethoxyanthracenes (**127**). By subjecting these anthracenes to a Diels–Alder reaction with benzyne generated from unsubstituted or dimethoxy anthranilic acid (**80** or **128**), triptycene derivatives methoxy-substituted at the 2,3,6,7- (**129**) or 2,3,6,7,14,15-positions (**130**) are obtained [46, 67–69]. Deprotection of these methoxy groups using boron tribromide yields the corresponding triptycene 2,3,6,7-tetrahydroxy (**131**) or 2,3,6,7,14,15-hexahydroxy (**132**) derivatives [46, 67–70]. Related hexahydroxytriptycene (**50**) devoid of alkyl substituents at the 9- and 10-positions (i.e., R^1 = H for **132**) was prepared from 2,3,6,7,14,15-hexabromotriptycene **45** (Fig. 3) [46]. The reaction of furan (**136**) with benzyne derived from the lithiation of substituted benzenes (**133**–**135**) yields 1,4-epoxy-1,4-dihydronaphthalene derivatives (**137**). These compounds undergo Diels–Alder reactions with hexa-substituted anthracenes (**127**) to yield epoxy products (**138**), which, through dehydration and demethylation by acid treatment, are transformed into highly substituted 2,3,6,7-tetrahydroxybenzotriptycene (**139**) [69, 70]. 2,3,6,7-Tetracyanotriptycene derivatives (**141**) were obtained by palladium-catalyzed cyanation of the corresponding triflated compound (**140**) derived from **131** [71]. Hydrolysis of the cyano groups of **141** yields 2,3,6,7-tetracarboxyltriptycene (**142**). The corresponding acid anhydride derivatives (**143**) were obtained by reacting with acetic anhydride [71]. An acid anhydride derivative devoid of alkyl substituents at the 9- and 10-positions (R^1 = H for **142**) can be synthesized by oxidation of

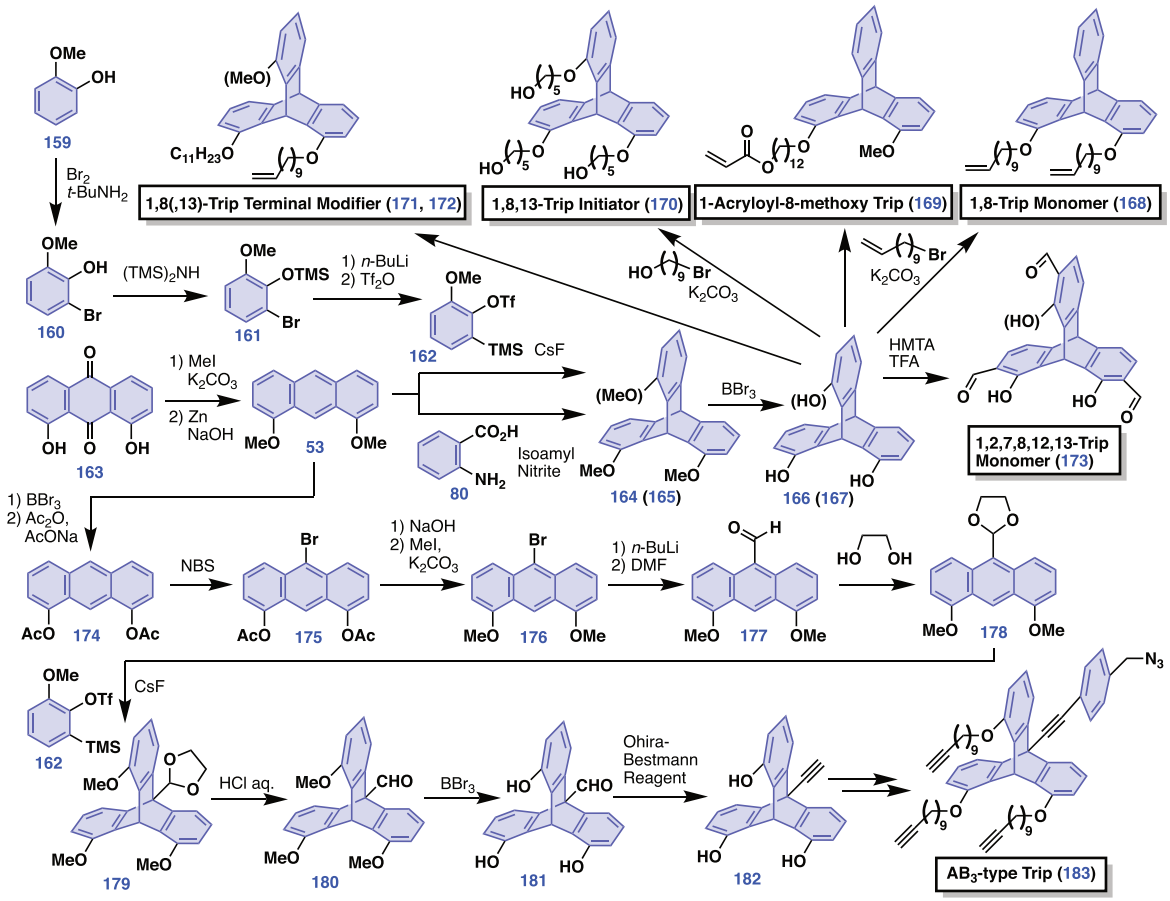

Fig. 8 Synthesis of 1,8,13-substituted trip-monomers

2,3,6,7-tetramethyltriptycene (**147**) using potassium permanganate [72]. 2,3,6,7-Tetramethylanthracene (**145**), the precursor of **147**, is obtained by a Friedel–Crafts reaction using *ortho*-xylene (**144**), dichloromethane, and aluminum chloride. The Diels–Alder reaction between **145** and benzyne yields **147**. Similarly, 2,3,6,7,14,15-hexamethyltriptycene (**148**) can be obtained using anthranilic acid with two methyl groups (**146**) instead of anthranilic acid (**80**) as a benzyne precursor. Compound **148** can be transformed to tri-acid anhydride **150** through successive oxidation (**149**) and intramolecular condensation [73]. 1,3,6,8-Tetramethylanthracene (**152**) can be prepared through a Friedel–Crafts reaction of *meta*-xylene (**151**) in dichloromethane [74]. 1,3,6,8-Tetramethyltriptycene (**153**) [74] and its monobenzoquinone derivative (**154**) [75] are obtained by the reaction of **152** with benzyne generated from anthranilic acid (**80**) and *para*-benzoquinone (**51**), respectively. Both **153** and **154** can be selectively nitrated at the 2,7-positions flanked by methyl groups (**155** [74] and **156** [75]) using a mixture of potassium nitrate and trifluoroacetic acid. Reduction of these nitrated products using hydrazine and metal catalysts yields 1,3,6,8-tetramethyl-2,7-diaminotriptycene (**157**) and 13,16-dihydroxy-1,3,6,8-tetramethyl-2,7-diaminotriptycene (**158**). The latter has been used as a building block for redox-active PIMs [75].

Figure 8 summarizes the synthesis of the 1,8,13-substituted triptycene derivatives. Our group reported that, through the Diels–Alder reaction of 1,8-dimethoxyanthracene (**53**) and benzyne generated from a methoxy-substituted precursor (**162**), 1,8,13-trimethoxytriptycene (**165**) can be prepared along with its 1,8,16-isomer as a minor product (1,8,13/1,8,16 = 2/1) [11]. Compounds **53** and **162** are synthesized in two steps from 1,8-dihydroxyanthraquinone (**163**) and in four steps from guaiacol (**159**), respectively. Similarly, 1,8-dimethoxytriptycene (**164**) can be obtained using **53** and benzyne [76]. By reacting these methoxy-substituted triptycenes with boron tribromide, we have shown that 1,8-dihydroxy and 1,8,13-trihydroxytriptycenes (**166, 167**) can be synthesized [11, 77]. A wide variety of substituents can be introduced to these hydroxylated derivatives *via* ether linkages, and the resulting alkoxytriptycenes have been found to exhibit particular 2D assembly properties [11, 77–81], which will be described in detail later. The various 1,8(,13)-substituted derivatives developed thus far include those with terminal olefin moieties (**168, 171, 172**) [77, 80, 81] and acryloyl groups (**169**)

[78]. Compounds **171** and **172** are used as end modifiers for polydimethylsiloxane (PDMS) [80, 81]. We also prepared a 1,8,13-triptycene initiator with hydroxy termini (**170**) [79]. Mastalerz et al. also reported a synthetic method for 1,8,13-trihydroxytriptycene **167** at approximately the same time and showed that the *ortho*-positions of its hydroxy groups can be formylated (**173**) by the reaction using hexamethylene tetraamine in the presence of trifluoroacetic acid [82]. From hexa-substituted monomer **173**, a triptycene-containing 3D COF was synthesized through the formation of a salphen complex [83].

The synthesis of bridgehead-substituted 1,8,13-triptycenes, which involves selective functionalization of the 10-position of 1,8-substituted anthracenes, requires somewhat laborious, multiple protection/deprotection steps [84]. Converting the methoxy groups of **53** to acetoxy groups (**174**) allows selective bromination at the 10-position using *N*-bromosuccinimide (NBS). The acetoxy groups of the resulting **175** were then converted back to methoxy groups. The synthesized 10-bromo-1,8-dimethoxyanthracene (**176**) is lithiated at the 10-position using *n*-butyllithium and subsequently treated with *N*,*N*-dimethylformamide (DMF), yielding 10-formyl-1,8-dimethoxyanthracene (**177**). A bridgehead-substituted 1,8,13-triptycene skeleton (**179**) can be synthesized by protecting the formyl group of **177** with ethylene glycol (**178**) and then treating it with in situ generated methoxybenzyne. Successive deprotection of **179** using hydrochloric acid and boron tribromide yields 10-formyl-1,8,13-trihydroxytriptycene (**181**) [84]. The formyl group of **181** can be converted to an ethynyl group (**182**) at this stage using the Ohira–Bestmann reagent [84]. Moreover, terminal ethynyl groups at this position are available for click reactions using copper(I) iodide and triethylamine [85]. The hydroxyl groups of **182** can be functionalized *via* etherification, and the remaining ethynyl group can be functionalized by nucleophilic substitution through acetylide or Sonogashira coupling. This protocol allows for the synthesis of bifunctional derivatives (**183**) carrying azide and terminal ethynyl groups [86]. This AB_3-type monomer was found to undergo polymerization in the assembled state, which will be discussed later. 1,8,13-Substituted triptycenes are relatively recently developed derivatives, and their synthesis has been thoroughly reviewed by Shindo et al. [87].

Recent progress in triptycene-containing polymers

Linear polymers

Here, we present some recent examples of triptycene-containing linear polymers with unique structures and interesting properties. Swager et al. reported the synthesis of polyethersulfone (**poly-1**) by polycondensation using 13,16-dihydroxy-1,8-dimethoxytriptycene (**55**), bisphenol A (**184**) and difluorodiphenylsulfone (**185**) (Fig. 9) [54]. The methoxy groups of **poly-1** were deprotected with boron tribromide to form **poly-2** with hydroxyl substituents, and bulky pyrazolium chloride (**186** and **187**) was attached to the hydroxyl groups to form a cross-linked network polymer (**poly-3**) with a structure in which the pyrazolium ions are densely aggregated (referred to as an ionic highway). Films of **poly-3** are reported to show both anion-conducting properties and high stability resulting from suppressed swelling due to its cross-linked nature.

Swager et al. synthesized a simple triptycene-containing polyethersulfone (**poly-4**) from 1,4-dihydroxytriptycene (**54**) and **185**, chloromethylated its triptycene moieties, and then treated the resulting **poly-5** with *N*-methylimidazole (**188**) to obtain **poly-6** with *N*-methylimidazolium chloride pendants (Fig. 10) [24]. This polymer not only forms anion exchange membranes for alkaline fuel cells but also provides a scaffold for metal nanoparticles [24, 88, 89]. For example, **poly-6** was composited with poly(4-vinylpyridine) and single-walled carbon nanotubes (SWCNTs), and the counter anion (Cl^-) was exchanged with tetrachloroaurate ($AuCl_4^-$). Upon treatment with sodium borohydride, small (<5 nm) gold nanoparticles (Au NPs) were formed in the composite film (Fig. 10). A field-effect transistor (FET) incorporating a Au NP composite layer was reported to serve as a chemo FET sensor for the detection of carbon monoxide and other gaseous molecules [88]. Moreover, bimetallic Pd/Pt nanoparticles (PdPt NPs) with a size of 1 nm can be synthesized within the **poly-6** film (Fig. 10). PdPt NPs react with hydrogen gas with high sensitivity in an oxygen atmosphere, and it has been reported that these materials can be applied as very sensitive hydrogen gas sensors [89]. In these systems, the use of triptycene units allows for the dense accumulation of functional groups as well as the formation of microporous structures.

Conjugated polymers derived from the 9,10-diethynylpentiptycene monomer **58** have been used as components of highly responsive chemosensors due to their porous nature [15]. Pentiptycene-containing **poly-7** with a benzothiadiazole unit composited with SWCNTs has been reported to serve as a sensor for the chemiresistive detection of solvent vapors such as benzene, toluene and xylene (i.e., BTX) (Fig. 11) [90]. Pentiptycene-containing **poly-8** with semiperfluoroalkyl side chains has been reported to function as a fluorescent polymer sensor for the detection of poly(-fluoroalkyl) substances (PFAS) (Fig. 11) [91].

Swager et al. reported that a palladium-catalyzed reaction between phenolic hydroxyl groups and aryl halides can be used in condensation polymerization to obtain a variety of

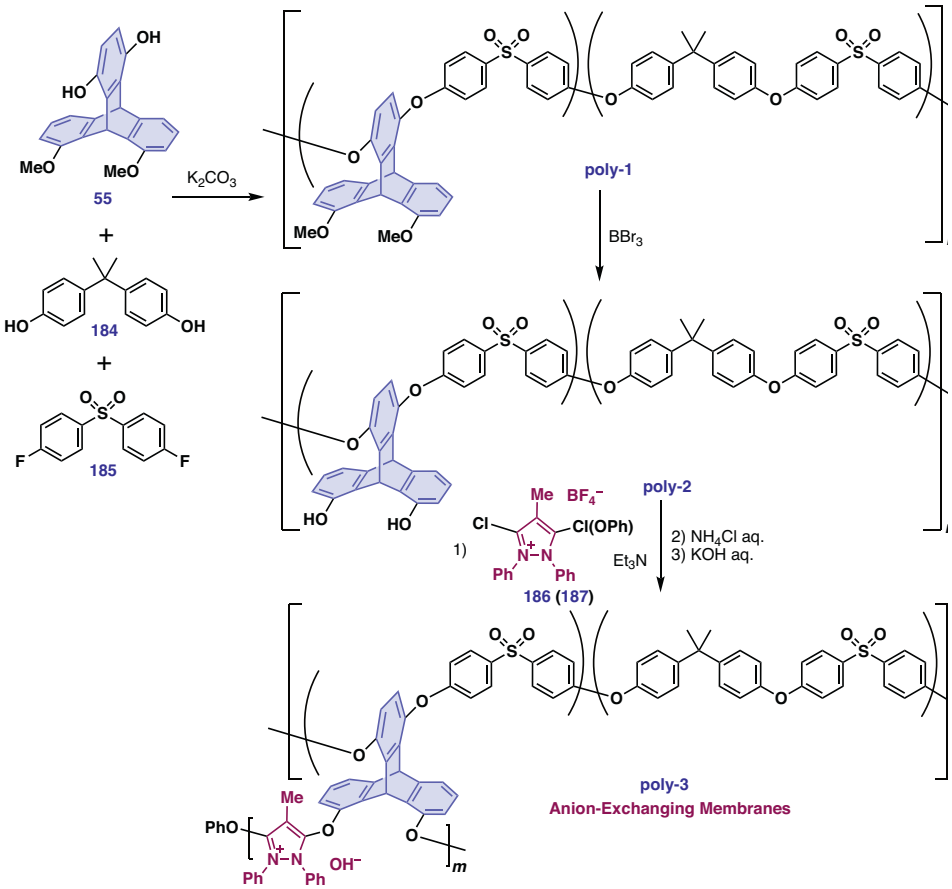

Fig. 9 Highly conductive and stable triptycene-containing anion-exchange polymer with an "ionic highway"

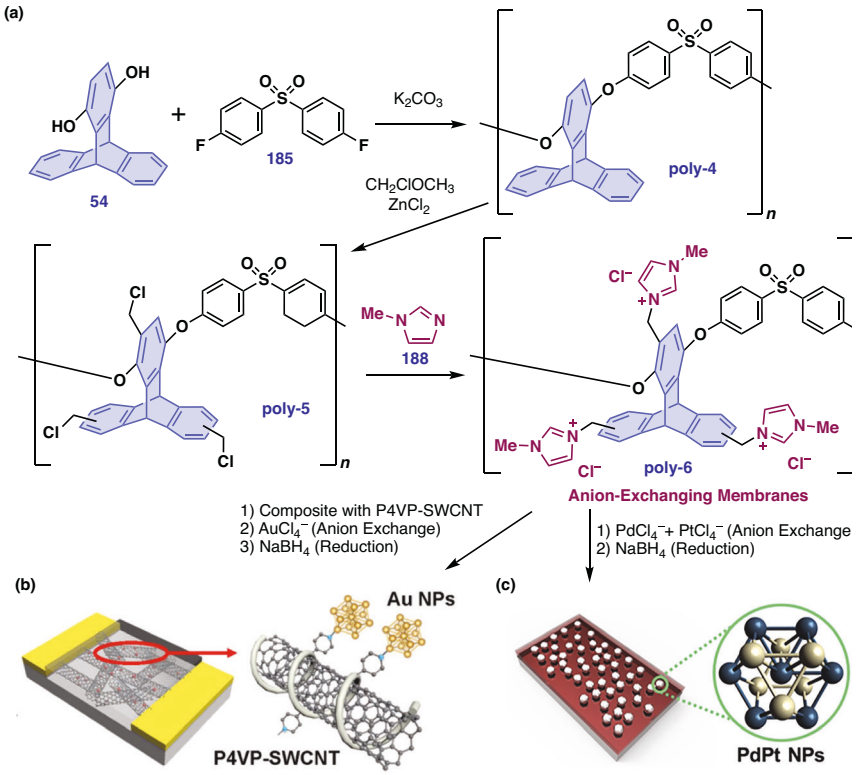

Fig. 10 **a** Synthesis of triptycene-containing anion exchange polymers and their application in (**b**) chemo-FET sensors (e.g., CO gas) and (**c**) H_2 gas sensors. **b** Adapted with permission [88] Copyright 2019, American Chemical Society. **c** Adapted under terms of the CC-BY 4.0 license [89] Copyright 2020, Elsevier

polyaryl ethers that cannot be synthesized through standard aromatic nucleophilic substitution methods (Fig. 12) [92]. Typically, 1,4-dihydroxy-6,14-di-*tert*-butyl-triptycene (**189**), 2,7-dibromospirobifluorene (**190**) and aromatic dibromides with various photocatalytically active sites (**191**–**196**) were reacted in the presence of a palladium catalyst (**197**) and a monophosphine ligand (**198**) to afford the corresponding polyethers (**poly-9**–**poly-16**). The obtained polymers are solution-processable and form microporous films that exhibit photocatalytic abilities, as shown in Fig. 12 [93]. A ruthenium catalyst can also be used to introduce perfluoroalkyl groups into the spirobifluorene moiety. The resulting polymer carrying fluorophilic side chains (**poly-9-$C_{17}F_{35}$**) can be used for the modification of the surface inside perfluoroalkoxy alkane (PFA) tubes. Using these modified PFA tubes, photoreactions can be conducted allowing the reagent to flow while irradiating with light [93].

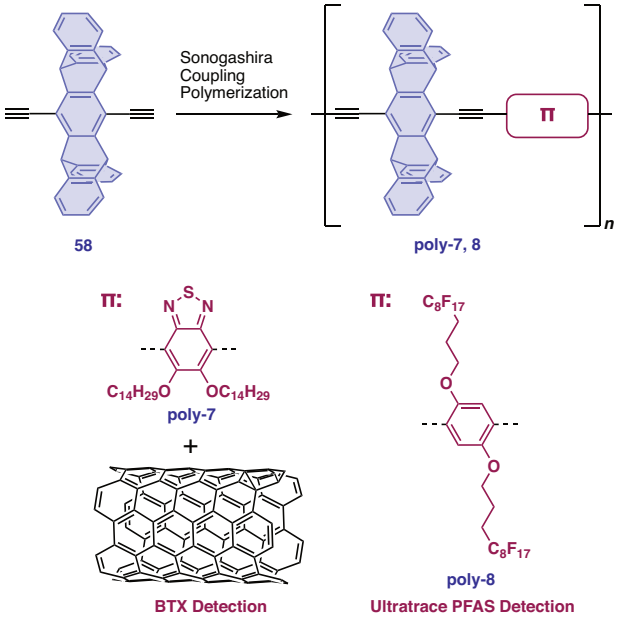

Fig. 11 Pentiptycene-containing π-conjugated polymers applied for chemosensing

Triptycene is widely used as a constituent in PIMs due to its rigidity and high intramolecular free volume (Fig. 13) [9, 18]. McKeown et al. reported dioxane-forming ladder polymerization using tetrafluoroterephthalonitrile (**199**) and 2,3,6,7-tetrahydroxybenzotriptycene with very bulky substituents (**139**) [69, 70]. The resulting **poly-17** was reported to exhibit highly selective gas permeability, significantly outperforming the 2008 Robeson upper bounds for O_2/N_2, H_2/N_2, CO_2/N_2, H_2/CH_4 and CO_2/CH_4 selectivities. Using a similar polymerization method, Guo et al. reported the synthesis of a ladder-type polymer (**poly-18**) with pentiptycene in the main chain from a tetrahydroxylated

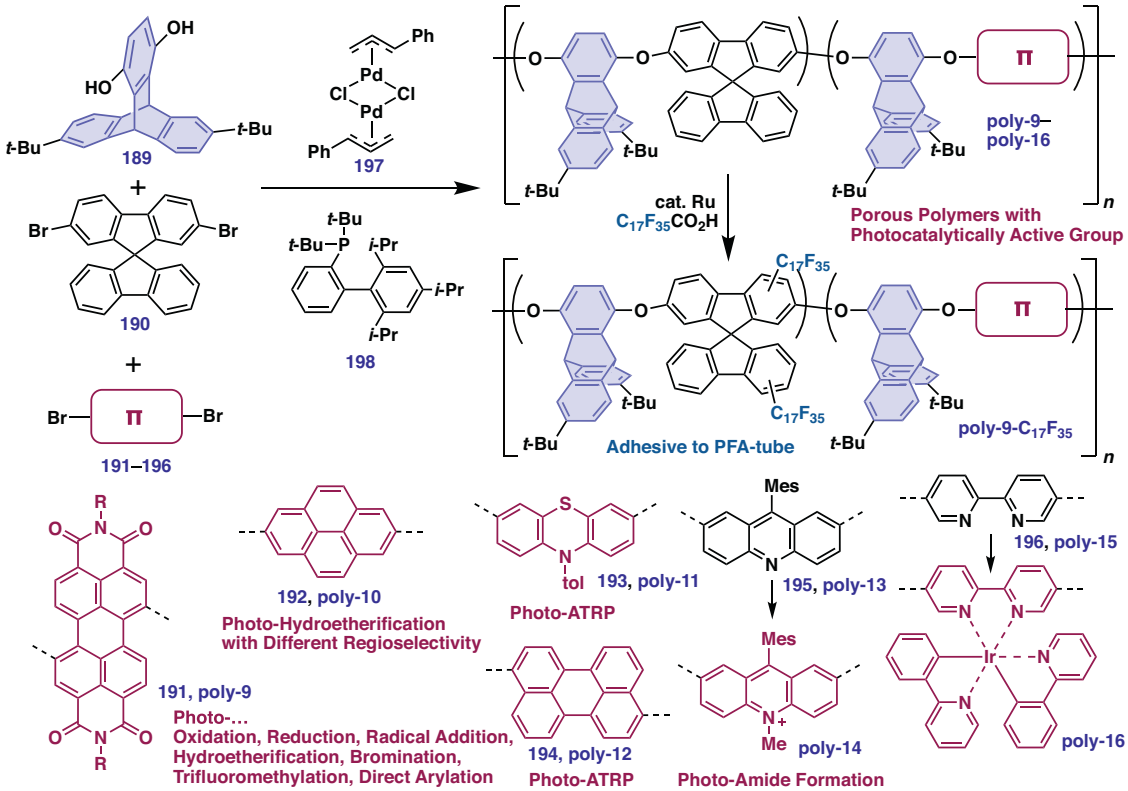

Fig. 12 Triptycene-containing solution-processable porous photocatalysts obtained by palladium-catalyzed carbon–oxygen bond formation

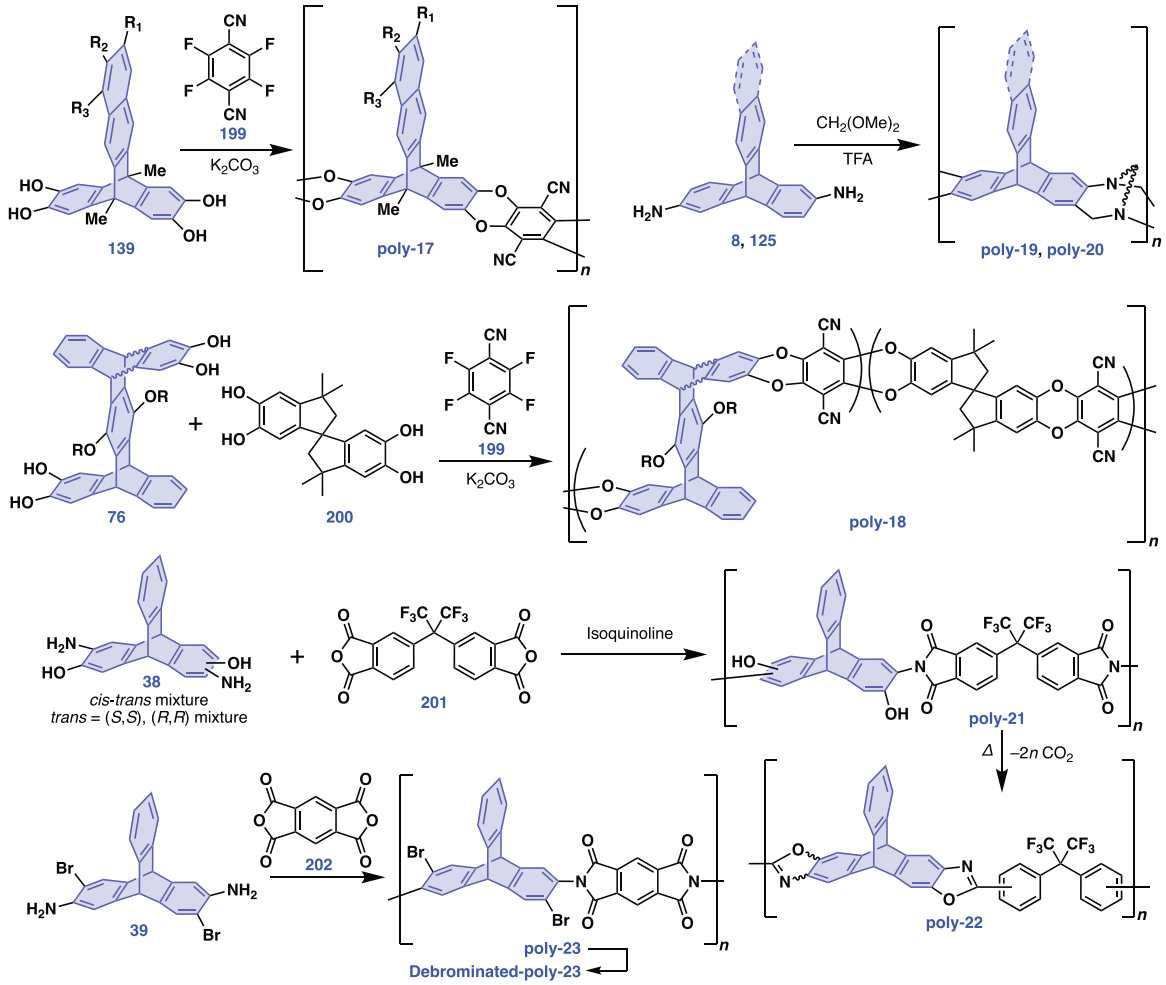

Fig. 13 Triptycene-containing PIMs useful in gas-separation membranes

pentiptycene (**76**), a tetramethyl spirobindan tetraol (**200**) and **201** [55]. High CO_2/CH_4 permselectivity was reported for **poly-18**. McKeown et al. also reported ladder polymerizations by the reaction of dimethoxymethane with 2,6-diaminotriptycene (**8**) and 2,6-diaminobenzotriptycene (**125**) to yield Tröger's base-containing PIMs **poly-19** [94] and **poly-20** [66], respectively. Condensation of a trip-monomer with two hydroxy groups and two amino groups (**38**) and 4,4'-(hexafluoroisopropylidene)diphthalic anhydride (**201**) in the presence of isoquinoline yielded polyimide **poly-21**, which, after thermal treatment, was transformed into thermally rearranged polybenzoxazole **poly-22** [36]. Li, Yi, Ma et al. reported that a polyimide membrane (**poly-23**) obtained from 2,6-diaminomonomer (**39**) with *ortho*-bromo groups and pyromellitic anhydride (**202**) showed *ca*. 8 times greater gas permeability than the corresponding polyimide devoid of bromo groups [38]. Moreover, when the **poly-23** membrane was heated to 550 °C, debromination occurred yielding a carbon molecular-sieve membrane, which displayed an almost 9-fold increase in gas permeability while maintaining permselectivity, with CO_2/N_2 and CO_2/CH_4 selectivities of 29.2 and 30.9, respectively, and an unprecedentedly high CO_2 permeability coefficient of 20639 barrer [38].

Gong, McKeown et al. developed a triptycene-containing polyimide **poly-24** with a hydroquinone moiety by reacting 13,16-dihydroxy-1,3,6,8-tetramethyl-2,7-diaminotriptycene (**158**) with pyromellitic dianhydride (**202**) in the presence of isoquinoline (Fig. 14) [75]. This polymer has a rigid and randomly contorted main-chain structure in which the rotation of the diimide unit is inhibited by the methyl groups on the triptycene moiety. Accordingly, **poly-24** shows excellent solubility in aprotic polar solvents and can be easily cast into freestanding films. Upon treatment with CAN, **poly-24** is oxidized to form the *para*-benzoquinone derivative **poly-25**, which undergoes a four-step redox process with excellent reversibility (Fig. 14). Lithium-ion battery cells using easily solution-processable **poly-24** as a component of the cathode material have been reported to exhibit stable cycling performance [75].

Despite the fact that many trip-monomers have chirality, there are only a few examples of optically active

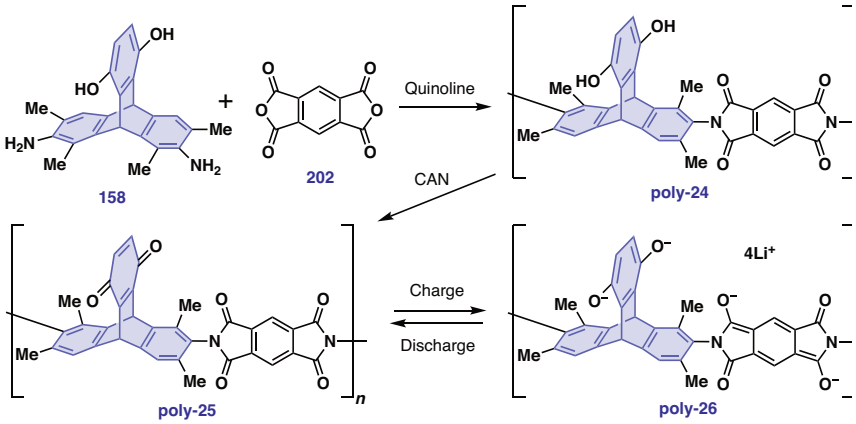

Fig. 14 Triptycene-containing redox-active PIMs useful as electrodes for lithium-ion batteries

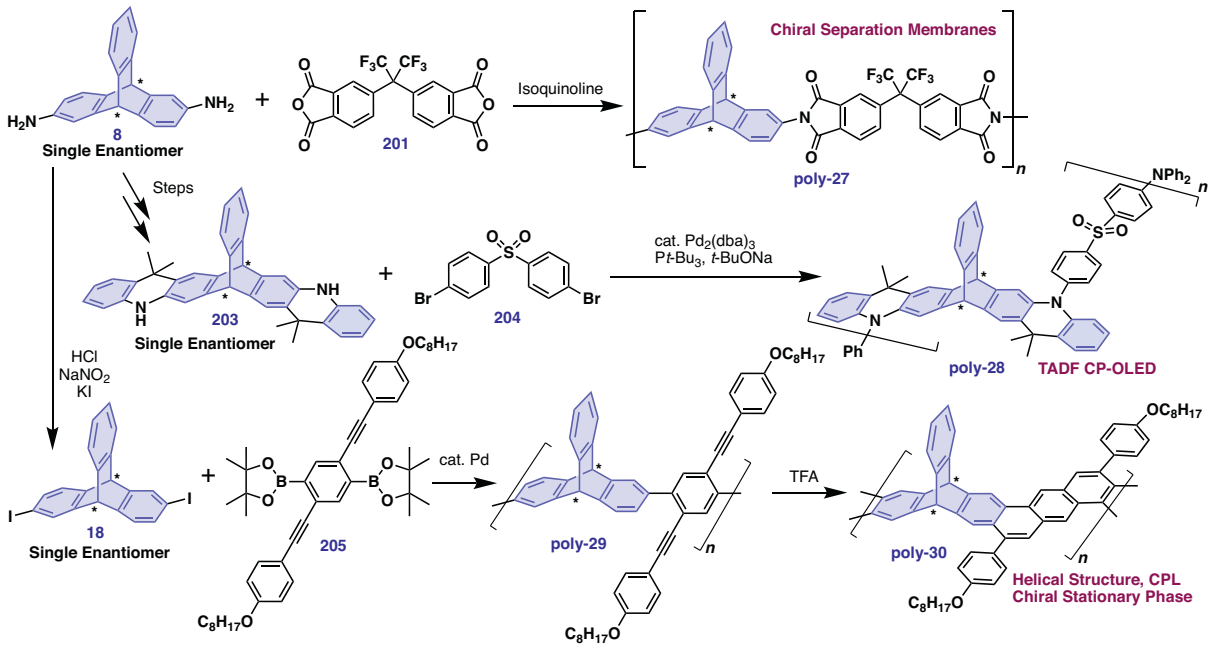

Fig. 15 Optically active triptycene-containing polymers

triptycene polymers [7, 31, 32]. Examples of the synthesis of such systems are shown in Fig. 15. The polycondensation of optically active 2,6-diaminotriptycene (**8**), which can be obtained by means of chiral HPLC, with acid anhydride 4,4'-(hexafluoroisopropylidene)diphthalic anhydride (**201**) in the presence of isoquinoline yields triptycene-containing polyimide **poly-27** [31]. This polymer serves as an optically active PIM, and its freestanding film can be used for enantioselective membrane separation. Chen et al. synthesized a chiral triptycene with dihydroacridine blades (**203**) from optically active **8** [95]. Compound **203** was then reacted with bis(4-bromophenyl) sulfone (**204**) in the presence of a palladium catalyst to produce optically active **poly-28**. This polymer shows thermally activated delayed fluorescence (TADF) properties, where the triptycene and sulfone moieties serve as electron donors and acceptors, respectively, and emits circularly polarized luminescence (CPL) with a dissymmetry factor (g_{lum}) on the order of 10^{-3} [95]. Using **poly-28**, circularly polarized organic light-emitting diodes (OLEDs) were successfully fabricated by means of solution processing. Ikai et al. synthesized optically pure 2,6-diiodotriptycene (**18**) from the corresponding optical isomer of **8** [96]. This was then used in a Suzuki coupling polymerization with ethynyl-substituted diboronic ester (**205**) to yield optically active **poly-29**. Upon treatment with trifluoroacetic acid, **poly-29** undergoes a geometrically selective Friedel–Crafts reaction, yielding the ladder polymer **poly-30**, whose conformation is fixed in a one-handed helical structure [96]. It has been reported that **poly-30** exhibits CPL and can be used as a stationary phase for chiral column chromatography.

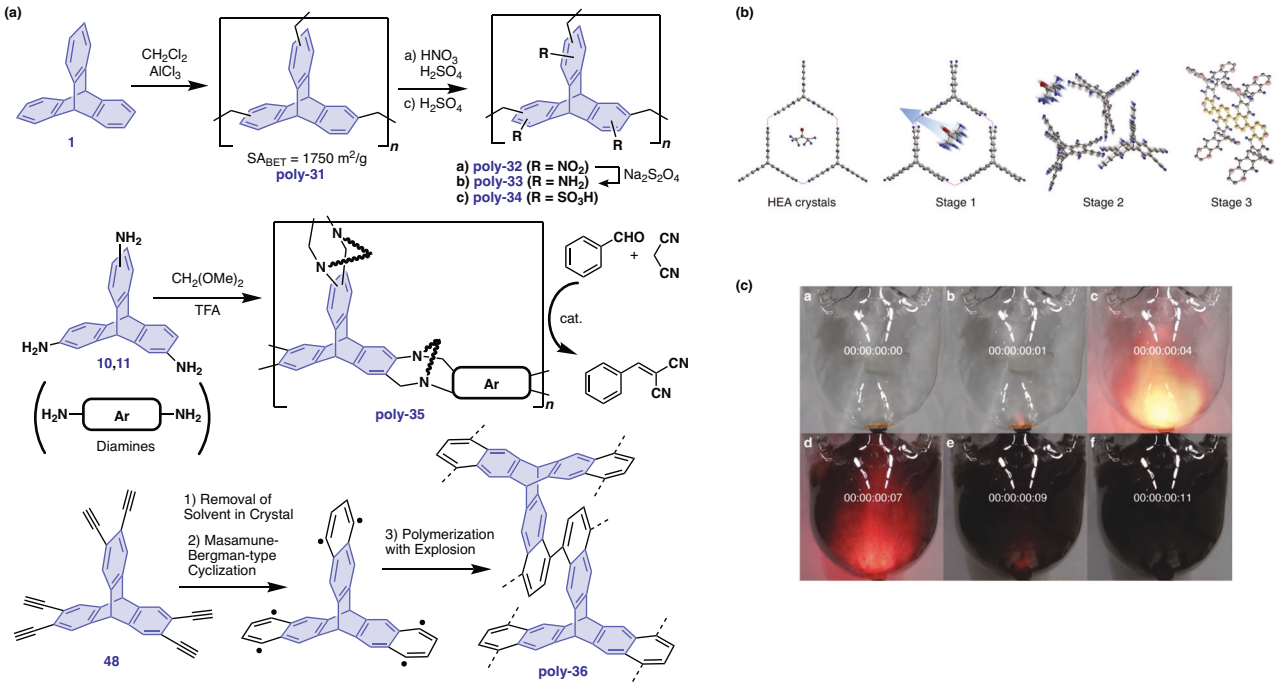

Fig. 16 **a** Selected examples of triptycene-containing nonregular network polymers. **b**, **c** Explosive reactions of **48** forming **poly-36** triggered by solvent desorption. **b**, **c** Adapted under terms of the CC-BY 4.0 license [45] Copyright 2017, Springer Nature

Network polymers

Triptycene can be easily tri- and hexa-functionalized by Friedel–Crafts-type reactions (Fig. 3). This approach is also useful for the synthesis of triptycene-containing network polymers; however, the resulting polymers are usually insoluble and devoid of regular structures. Many examples of this type of polymer have been described in a recent review by C-F. Chen et al. [8], so only selected examples are presented here (Fig. 16). McKeown et al. reported that porous 3D network polymers (**poly-31**) with a Brunauer–Emmett–Teller (BET) specific surface area (S_{BET}) of 1750 m^2/g can be obtained by the reaction of unsubstituted triptycene (**1**) with dichloromethane in the presence of aluminum trichloride (Fig. 16a, top) [97]. Furthermore, **poly-31** can be easily functionalized with nitro (**poly-32**), amino (**poly-33**), or sulfo (**poly-34**) groups [98]. McKeown et al. synthesized a Tröger's base-containing network polymer (**poly-35**) by the reaction of 2,6,14- or 2,7,14-triaminotriptycene (**10, 11**) with dimethoxymethane in the presence of trifluoroacetic acid (Fig. 16a, middle). They found that **poly-35** serves as a base catalyst for the Knoevenagel condensation of benzaldehyde and malonitrile [99]. Moreover, the use of various diamines for copolymerization with triaminotoriptycene allows for tuning of the pore size and catalytic activity of the resulting network polymers [100]. Baek et al. reported a very unique solid-state polymerization of triptycene derivatives [45]. They found that 2,3,6,7,14,15-hexaethynyltriptycene (**48**) forms stable crystalline materials that incorporate acetone and water molecules, but rapid heating causes desorption of the solvent. This triggers Masamune–Bergman cyclization of the *ortho*-diethynyl moiety to generate highly reactive radicals, leading to explosive reactions and the formation of **poly-36** with a porous structure (Fig. 16b, c).

Porous 2D polymers

Triptycene derivatives that undergo porous 2D hexagonal packing typically have structures with blades laterally extended through the 2,3-, 6,7- and 14,15-positions (Fig. 1). In 2014, King et al. reported a triptycene derivative (**206**) with photoreactive tetrafluoroanthraceno blades (Fig. 17a, left and center) [101]. This extended triptycene derivative forms porous hexagonal packing in the crystalline state, with a configuration in which the tetrafluoroanthraceno blades are intermolecularly π-stacked (Fig. 17b, left). Then, light irradiation was used to induce [4+4] cycloadditions between the blades, with photoirradiation (460 nm) of a single-crystal sample at 223 K leading to dimerization (**207**) (Fig. 17b, center) and further photoirradiation at 400 nm forming a 2D polymer (**poly-37**) (Fig. 17b, right). This two-step photochemical reaction proceeds in a single-crystal-to-single-crystal manner. It has been reported that crystalline samples of this 2D polymer can be exfoliated to monolayer sheets by heating to 50 °C in *N*-methyl-2-pyrrolidone (NMP). Before this study, the same group reported in 2013 that light irradiation of single crystals of a derivative with

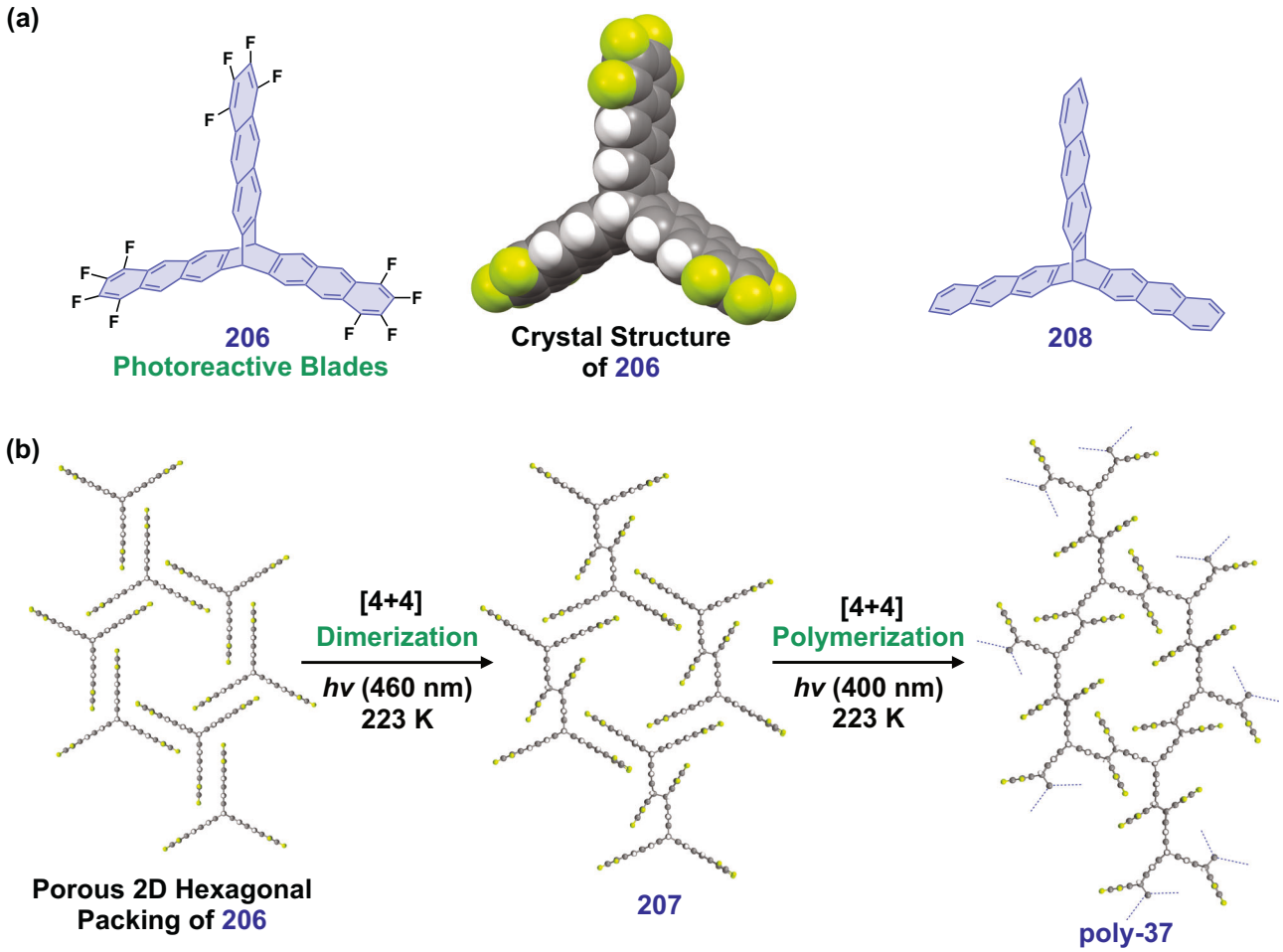

Fig. 17 **a** Molecular structures of **206** and **208**, which feature photoreactive tetrafluoroanthraceno and anthraceno blades, respectively. **b** Schematic illustrations of the two-step single-crystal-to-single-crystal transformations of **206** into its 2D polymer **poly-37**

nonfluorinated anthraceno blades (**208**) produced a 2D polymer (Fig. 17a, right) [102]. However, the photopolymerization of **208** was reported to be "not single-crystal to single-crystal transformation". In 2021, Lackinger et al. reported that vacuum deposition of **206** on a hexacosane-passivated graphite substrate followed by thermal annealing produced a crystalline monolayer film (with a domain size of up to 500 nm) consisting of a porous hexagonal lattice similar to that of a single crystal [103]. When this monolayer sample is irradiated with light using a high-power LED, on-surface photocycloadditions proceed, yielding a 2D polymer.

Based on a similar molecular design, King et al. reported the formation of Langmuir–Blodgett (LB) films at the air/water interface using triptycene derivative **209**, which contains a hydrophilic diethylene glycol moiety at the bridgehead position that serves as an anchor for the water layer (Fig. 18a) [104]. A chloroform/hexane solution of **209** was spread on the air/water interface and compressed at 1 °C using an LB trough, and the mean molecular area (MMA) was calculated from the compression isotherm. Phase changes were observed at approximately 155–135 and 80 $Å^2$, and the former MMA was assigned to porous hexagonal *p*6 packing. STM measurements of a LB film of **209** transferred onto a HOPG substrate show a porous structure that is consistent with the simulated pattern (Fig. 18b). Upon irradiation with 365 nm light, the LB film of **209** underwent photopolymerization, and the obtained thin-film polymer was found to be mechanically hard enough to deform a paper Wilhelmy plate during the Langmuir experiment.

Similar to **209**, several amphiphilic extended triptycene derivatives have been reported to form highly ordered LB films with porous hexagonal structures (**210** [105], **211** [106] and **212** [106], Fig. 18c). Schlüter et al. reported the synthesis of 2D polymers using **211, 212** and a 1:1 mixture of **211** and **212** using the LB technique and light irradiation [106]. After being transferred onto a Au(111) substrate, the obtained 2D polymers were characterized by tip-enhanced Raman spectroscopy (TERS), which allowed for the evaluation of the conversion number (*X*) of the crosslinked structures (i.e., anthracene dimer moieties). The results

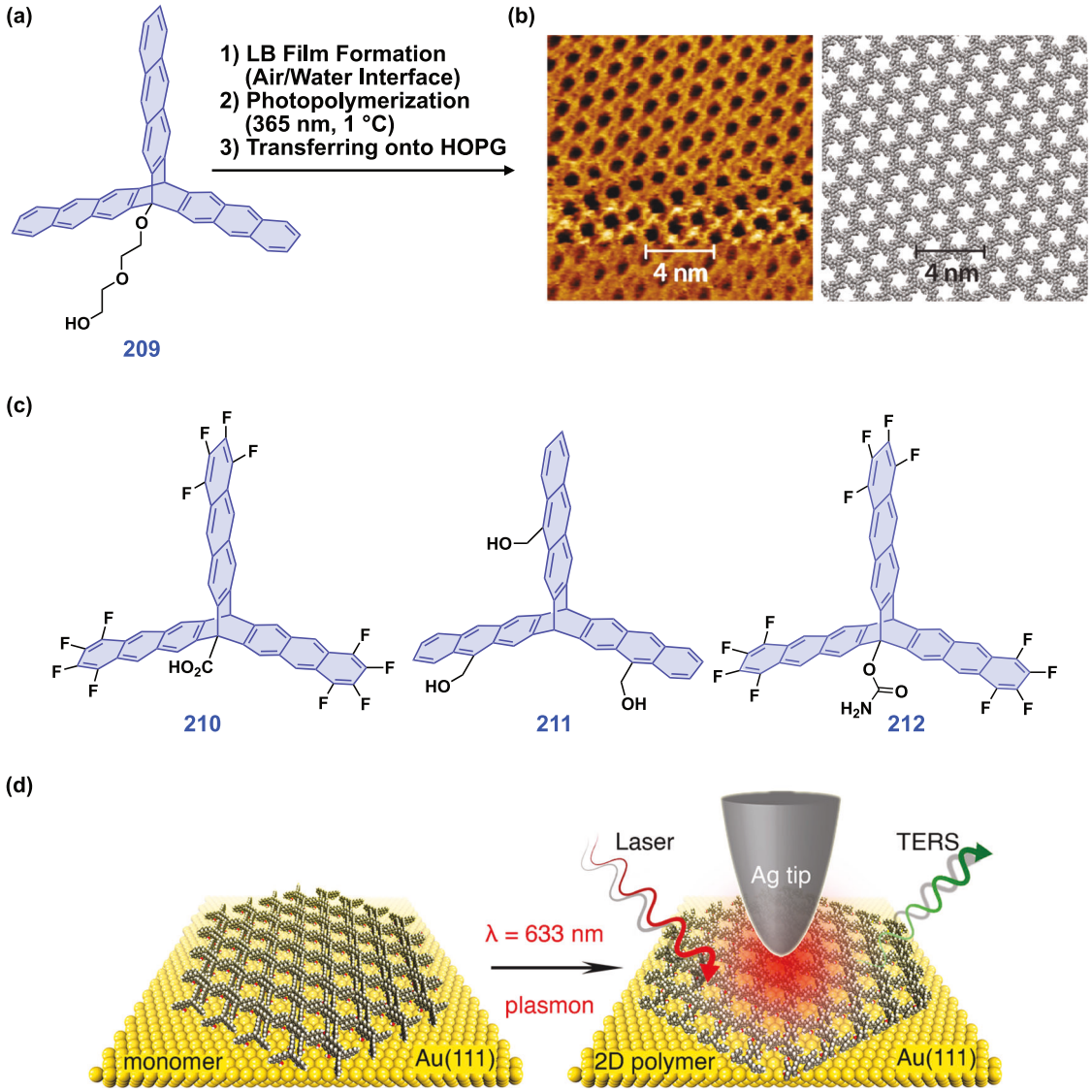

Fig. 18 **a** Formation of a LB film composed of amphiphilic propeller-shaped **209**, which carries a diethylene glycol chain that anchors the molecule to the water surface. **b** STM image (left) and simulated *p*6 lattice of **209** (right). **c** Structures of a series of amphiphilic propeller-shaped molecules (**210, 211,** and **212**) designed for the formation of structurally well-defined LB films and their crosslinked 2D polymers. **d** Schematic illustration of plasmon-induced [4+4]-cycloaddition/2D polymerization of LB films **210** and **211**. **b** Adapted with permission [104] Copyright 2015, American Chemical Society. Adapted under terms of the CC-BY 4.0 license [107] Copyright 2021, Springer Nature

showed high conversion numbers, with averages of $X = 87.7 \pm 1.8$ (**211**), 92.0 ± 1.7 (**212**), and $94.1 \pm 2.1\%$ (copolymer). Based on these values, along with the random-growth model, the calculated crystallinities of the 2D polymers were 95.8 ± 1.2, 98.2 ± 1.1 and $99.0 \pm 1.4\%$ for **211, 212** and **211/212** (1/1), respectively. In 2021, Shao, Lan, Zenobi, and coworkers performed TERS measurements on LB films of **210** and **211** transferred onto Au(111) substrates using silver chips and found that visible laser irradiation (633 nm) caused intermolecular [4+4] cycloadditions between the blades in the 2D assembly as plasmon-induced chemical reactions (PICRs) (Fig. 18d) [107].

Nonporous 2D assemblies and polymers

Triptycene derivatives that form dense and nonporous 2D hexagonal packing are characterized by structures in which substituents are introduced at either the 1,8,13- or 4,5,16-positions (Fig. 1). In derivatives with these substitution patterns, the free volume around the triptycene backbone can be retained, which is favorable for the formation of 2D nested packing. In fact, most triptycene derivatives reported to form nonporous 2D hexagonal structures in crystals or in the liquid-crystalline state have these substitution patterns [87, 108]. It has been found that 1,8,13-substituted tripty-

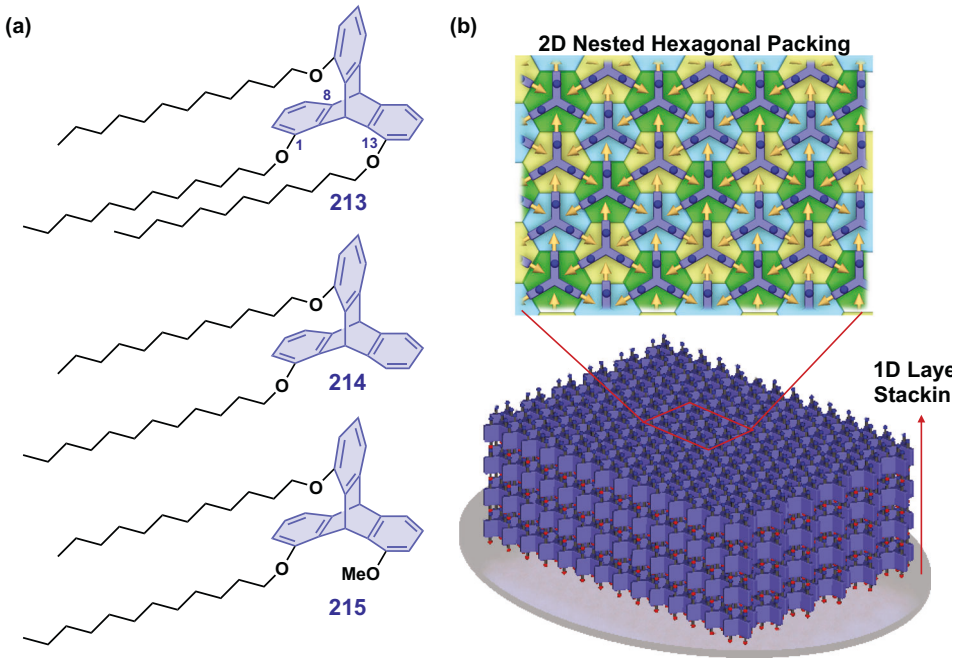

Fig. 19 **a** Molecular structures of 1,8(,13)-substituted triptycene derivatives **213**–**215** having alkoxy side chains. **b** Schematic illustrations of a "2D nested hexagonal packing + 1D layer stacking" structure formed by the self-assembly of **213**–**215**

cene derivatives can exhibit 2D assembly ability even when another substituent is introduced at the bridgehead position (*vide infra*). Note that unsubstituted triptycene (**1**) does not form nested packing in the crystal or on the substrate surface [109, 110]. Therefore, it is essential to choose appropriate substituents and substitution patterns to realize dense 2D hexagonal assemblies.

With the aim of constructing large-area, highly ordered organic thin films through molecular self-assembly, our group developed a tripodal triptycene (**213**) with long-chain alkoxy groups introduced at the 1,8,13-positions (Fig. 19a) [11]. In the bulk state, this compound forms a "2D nested hexagonal packing + 1D layer stacking" structure (Fig. 19b). The assembly of **213** on a solid substrate yields oriented thin films with 2D hexagonal sheets stacked parallel to the substrate (Fig. 19b) on a variety of inorganic and polymer substrates simply by, e.g., spin-coating or vacuum deposition [11, 111, 112]. Importantly, in thin films of **213**, the ordered structure formed on nanometer-length scales can propagate to macroscopic length scales. For example, in through-view XRD measurements of a vacuum-deposited film of **213** (50 nm in thickness) formed on a sapphire substrate (2.0 cm in diameter), the in-plane azimuthal angle dependence of the peak intensity originating from the 2D hexagonal lattice does not change when the measurement position on the film is changed [11]. This observation indicates that the orientation of the 2D hexagonal lattice is aligned across the entire film.

Derivatives with different alkoxy chain lengths and those with only two or one long-chain alkoxy group also form 2D +1D structures similar to that of **213**, whereas their thermal stability largely depends on the triptycene substitution pattern (Fig. 19a) [11, 113]. For example, the 2D+1D assembly of 1,8-bis(dodecyloxy)tripycene **214** (m.p. 134 °C) shows significantly lower thermal stability than that of **213** (m.p. 211 °C). However, the assembly of 1,8-bis(-dodecyloxy)-13-methoxytriptycene **215**, in which one of the long-chain alkoxy groups in **213** is replaced by a methoxy group, exhibits greater relative thermal stability (m.p. 231 °C). These differences are directly reflected in the properties of the soft materials incorporating the triptycene units (*vide infra*).

Tripodal triptycenes are also useful as components in organic electronic devices [113–117]. We have found that the performance of flexible organic thin-film transistor devices can be significantly improved by forming several layers of **215** on the surface of a parylene-based polymer dielectric layer [114–117]. This triptycene-based surface modifier covers structural defects on the surface of the polymer substrate and lowers and homogenizes the surface energy. This leads to improved crystallinity of the organic semiconductor on the dielectric layer and overall performance of the transistors. Although SAMs can be used for the surface coating of inorganic substrates, they cannot be applied to polymer substrate surfaces. Tripodal triptycenes, which can form highly ordered and perfectly oriented films regardless of substrate type, provide a powerful tool for improving the performance of organic electronic devices.

Importantly, tripodal triptycenes exhibit excellent 2D assembly ability even when various functional groups are incorporated [84, 86]. For example, compound **216**, in which a sterically bulky spherical C_{60} is introduced *via* an

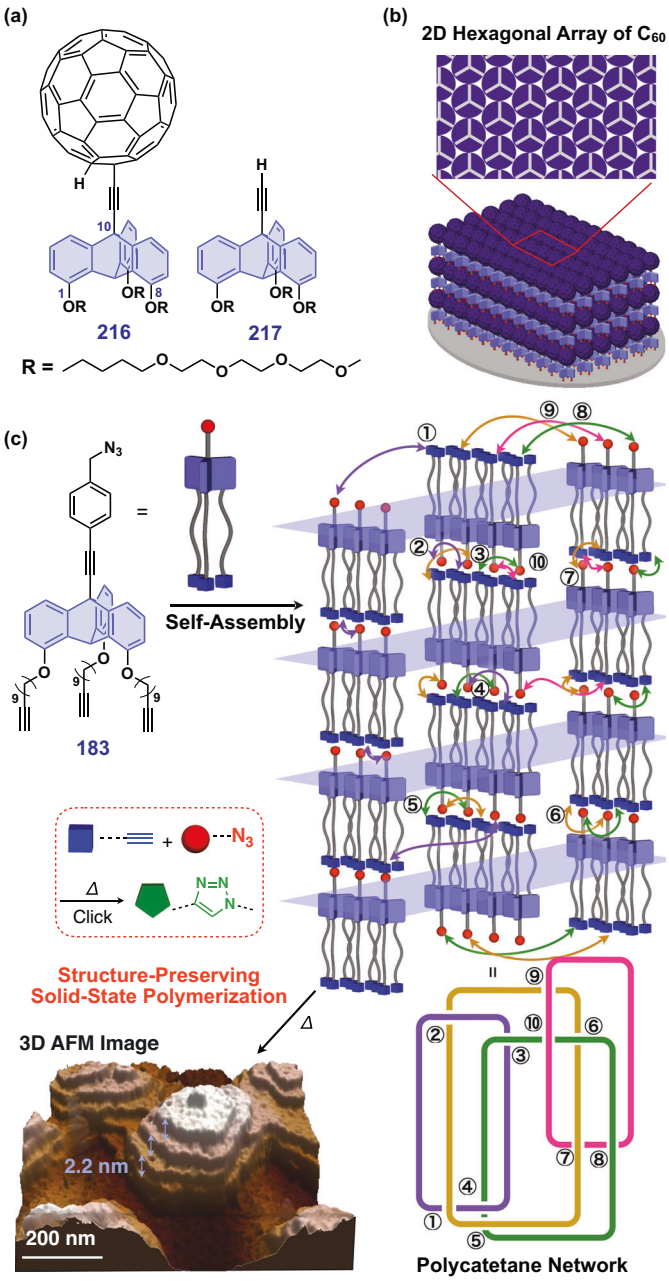

Fig. 20 **a** Molecular structure of C_{60}-appended tripodal triptycene **216** and its precursor **217**. **b** Schematic illustrations of the 2D+1D structure formed by the self-assembly of **216**. **c** Molecular structure (left) and schematic assembly structures of **183** before and after catalyst-free thermal Huisgen cycloaddition

ethynyl group at the bridgehead position, as well as its precursor **217** with a terminal ethynyl group (Fig. 20a), also forms 2D+1D structures in the bulk state [84]. The spin-coated thin films of **216** are oriented similarly to those of **215**, with a 2D+1D structure consisting of 2D layers of densely arranged C_{60} units (Fig. 20b). Time-resolved microwave conductivity (TRMC) measurements of these thin films revealed the anisotropic conduction of photo-carriers in the in-plane direction. Thus, tripodal triptycenes are useful supramolecular scaffolds [118] that promote the 2D assembly of various functional groups and molecular units, making it possible to improve their anisotropic properties. Face-selective introduction of an azide group and three terminal ethynyl groups into a tripodal triptycene (**183**) also leads to assembly into a 2D+1D structure both in the bulk state and on solid substrates (Fig. 20c) [86]. When this assembly is heated, intermolecular uncatalyzed Huisgen cycloadditions maintain the assembly structure. The resulting polymer is insoluble and possibly composed of a highly entangled polycatenane-like cyclic structure (Fig. 20c). The solid-phase polymerization of the oriented film of **183** proceeded while retaining the surface nano-terraced structure.

The incorporation of 1,8,(13)-substituted triptycenes into polymers induces long-range ordered structures through 2D assembly of the triptycene units, greatly

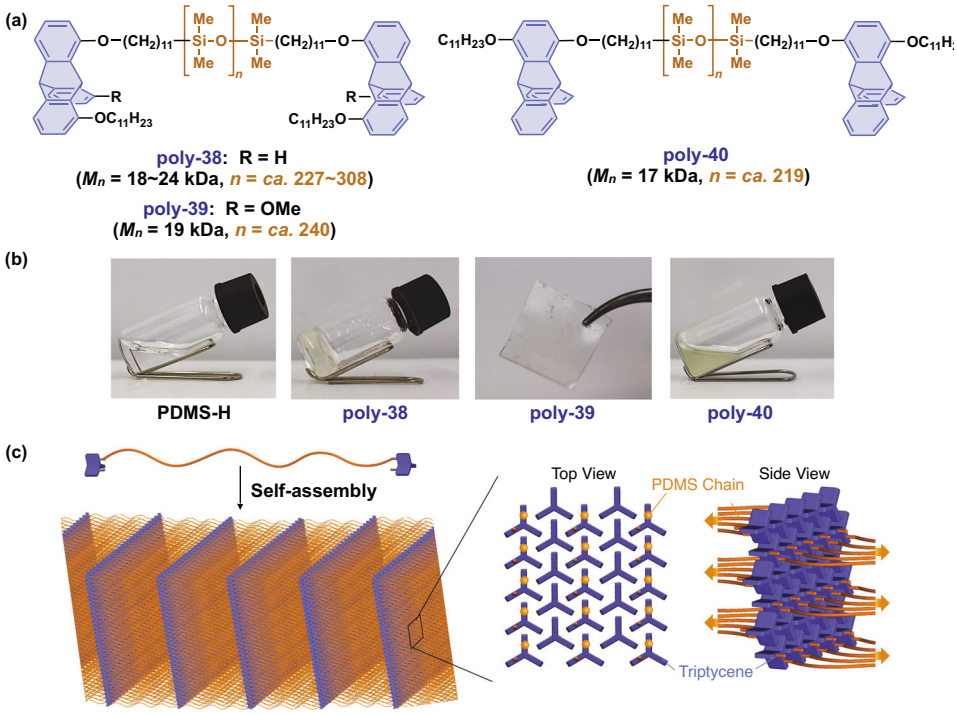

Fig. 21 **a** 1,8(,13)-Substituted triptycene-containing telechelic polymers **poly-38** and **poly-39** and 1,4-substituted triptycene-containing **poly-40**. **b** Photographs of bulk samples of PDMS-H and the telechelic polymers. **c** Schematic illustrations of the assembly structures of the telechelic polymers

enhancing the mechanical properties of the polymers [77–80]. Such specific 2D assembly can be achieved by incorporating the triptycene units at various sites of polymers, including at both ends [80, 81], in the main chain [77], side chains [78] and at various branch points [79]. Figure 21a shows the chemical structures of poly(-dimethylsiloxane) (PDMS) derivatives (**poly-38**–**poly-40**) with 1,8(,13)-triptycene units at both ends (**poly-38** and **poly-39**) along with a 1,4-substituted derivative (**poly-40**). For example, hydrosilylation of olefin-appended 1,8-substituted triptycene **171** (Fig. 8) with hydride-terminated PDMS (PDMS-H, M_n = 18 or 24 kDa) affords **poly-38** [80]. In sharp contrast to liquid PDMS-H, the telechelic polymer **poly-38** forms a highly viscous solid that exhibits birefringence (Fig. 21b). Rheological measurements revealed that the complex viscosity of **poly-38** (approximately 10^5 Pa·s) is 10^4 times greater than that of PDMS-H (approximately 10^1 Pa·s). Small- and wide-angle XRD measurements revealed that **poly-38** forms a 2D+1D structure with long layer spacings of 18–20 nm, in which 2D sheets of terminal triptycene units are stacked one-dimensionally via PDMS domains (Fig. 21c). Telechelic **poly-39** synthesized from 1,8,13-substituted triptycene **172** (Fig. 8) also forms a 2D+1D structure but has an even greater mechanical strength than **poly-38** and behaves as a thermoplastic, resulting in a freestanding film without any covalent cross-linking (Fig. 21b) [81]. It has also been shown that **poly-39** films exhibit self-healing properties. The only structural difference between **poly-39** and **poly-38** is the presence or absence of a methoxy group at the 13-position of the terminal triptycene units, and it is thus surprising that such a tiny change in substituent relative to the entire polymer has a significant impact on the mechanical and thermal properties. Moreover, the structural and physical properties of PDMS are largely unchanged in **poly-40** (Fig. 21a, b, right), where 1,4-substituted triptycene units without 2D assembly ability are introduced at both ends of the PDMS.

Ring-closing metathesis of 1,8-olefin-appended **168** (Fig. 8) yields macrocyclic olefin monomer **218**, which has been used for the synthesis of main chain-type triptycene-containing polymers (Fig. 22) [77]. We synthesized the homopolymer **poly-41** by ring-opening metathesis polymerization of **218** and the copolymer **poly-42** by copolymerization of **218** with cyclooctene [77]. Both **poly-41** and **poly-42** form 2D hexagonal sheet structures with triptycene units and lamellar structures filled with polymer chain domains, which leads to a marked improvement in the mechanical properties of the polymers. In **poly-43** without 2D assembly ability, no improvement in physical properties was observed [77]. While the triptycene polymers **poly-44** and **poly-45**, which have oligosiloxane- and ester-based main chains, respectively, also form 2D+1D structures, the urethane-containing **poly-46** does not (Fig. 22) [77]. Presumably, the hydrogen bonding ability of the urethane group may be superior to the assembling ability of the triptycene, hampering structural ordering of the polymer.

We synthesized diblock (**poly-47**), ABA triblock (**poly-48**) and random (**poly-49**) copolymers by reversible addition-fragmentation chain-transfer (RAFT) polymerization of

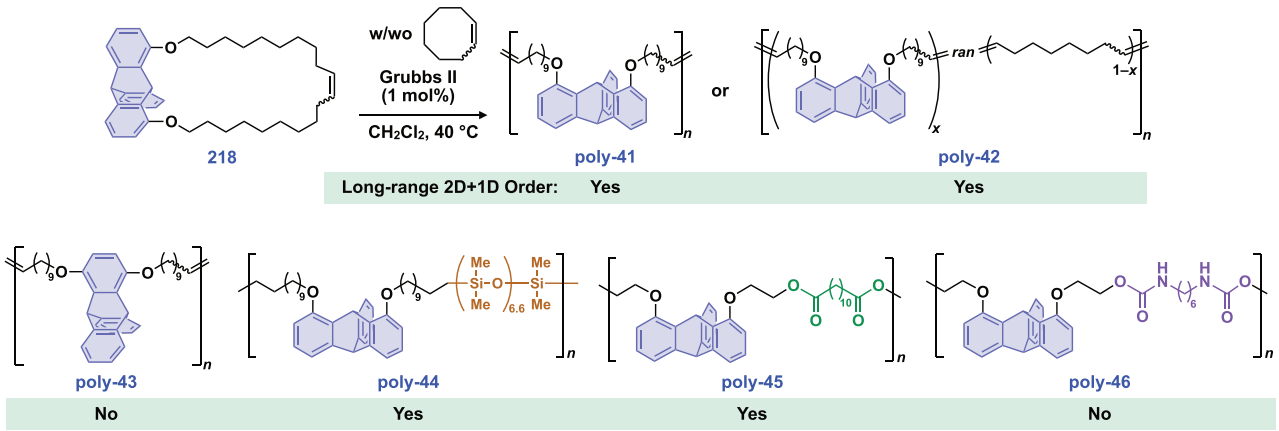

Fig. 22 Polymers incorporating 1,8-substituted triptycene units (**poly-41, poly-42, poly-44**–**poly-46**) in the main chains with a 1,4-substituted unit (**poly-43**)

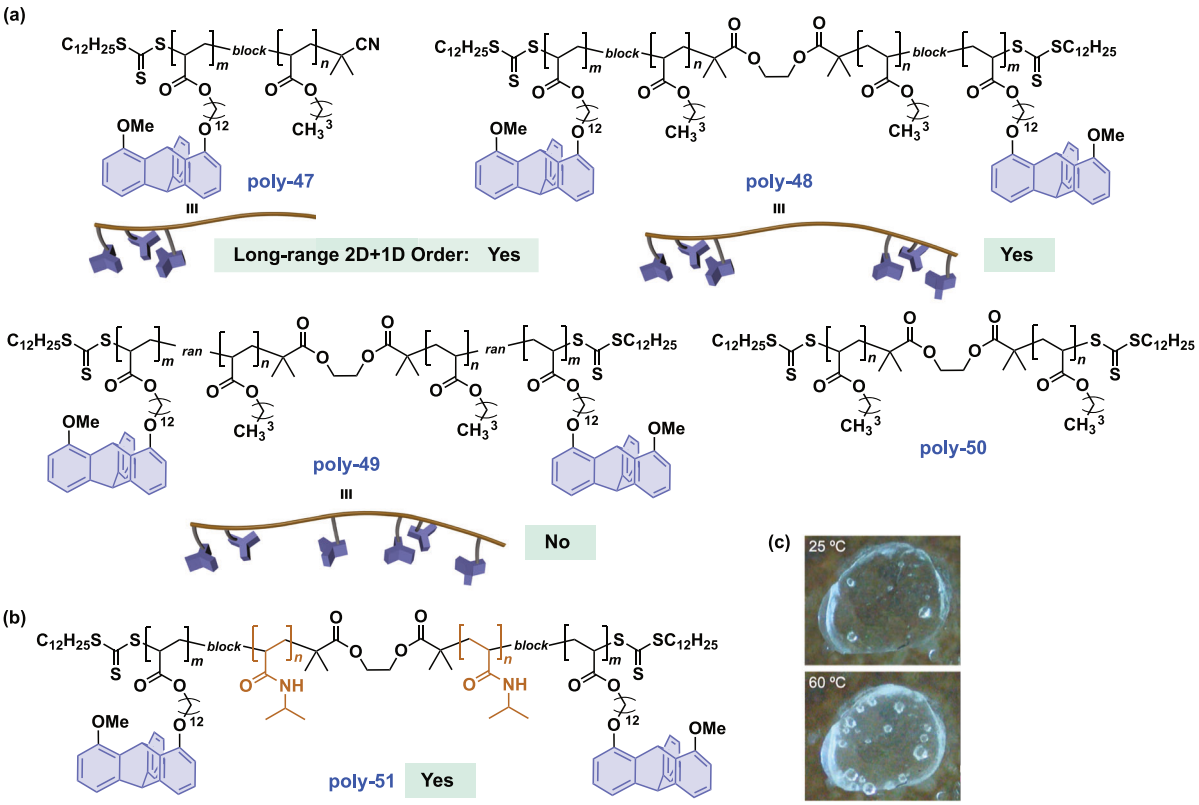

Fig. 23 **a** Molecular and schematic structures of diblock **poly-47**, ABA triblock **poly-48,** and random **poly-49** carrying 1,8-substituted triptycene-based side chains as well as **poly-50**, a precursor of **poly-48**. **b** Molecular structure of ABA triblock polymer **poly-51** with a PINIPAM segment and (**c**) photographs of its hydrogel. **c** Adapted with permission [78] Copyright 2023, American Chemical Society

1-acryloyl-8-methoxytriptycene **169** (Fig. 8) and n-butyl acrylate (Fig. 23a) [78]. The thermal stability of these triptycene-containing copolymers is comparable (2% weight loss temperature: *ca*. 300 °C) to that of the precursor polymer (**poly-50**) without triptycene units. However, while poly(*n*-butyl acrylate) derivatives, including **poly-50**, are liquids, the copolymers are all viscous solids. For diblock **poly-47**, both the melting (T_m) and crystallization (T_c) temperatures shift toward higher values with increasing triptycene content. While their triptycene contents are comparable, diblock **poly-47** has slightly greater T_m and T_c values than triblock **poly-48**, whereas the enthalpy changes associated with the phase transitions are in the same range. XRD measurements revealed that both diblock and triblock copolymers form

2D+1D structures with long-range ordering. In contrast, the random copolymer **poly-49** does not form a 2D+1D structure and shows no clear phase transition. It is worth noting that rheological measurements show that diblock **poly-47** and triblock **poly-48** exhibit complex viscosities 10^4–10^5 times greater than that of random **poly-49** over a wide temperature range. Therefore, in the design of side-chain-type triptycene polymers, the presence of block segments is essential for achieving long-range ordering. Accordingly, we designed **poly-51** with triptycenes at both ends of a poly(*N*-isopropylacrylamide) (PNIPAM) segment (Fig. 23b) [78]. This triblock copolymer yields hydrogels (60 wt% water content) without chemical cross-linking due to the formation of a 2D+1D structure with a 2D triptycene sheet and a hydrated PNIPAM domain. The hydrogel became turbid at 60 °C, and the PNIPAM domain exhibited a lower critical solution temperature (LCST) upon increasing the temperature. VT-XRD measurements of the hydrogel revealed that the interlayer distances decreased with increasing temperature while maintaining the 2D structure. These findings are expected to be applied to the future development of soft actuators that exhibit anisotropic motion in response to stimuli.

Conclusions

As outlined in this review, triptycene is a versatile scaffold that can be exploited by introducing a number of substituents in various patterns at its blades and bridgehead positions. It is also possible to impart characteristic redox properties to the blade sites. One of the main topics in the development of triptycene-based functional materials, diverse polymers, and molecular assemblies is the design of nanospaces (microporosity) in the assembly state, which is being explored for use in guest recognition, material transport, separation, and catalysis. Rigid three-bladed propeller molecules are suitable for forming porous or nonporous 2D lattices, and they provide excellent building blocks for forming 2D sheet structures that are not easily accessible. Their ability to form dense 2D sheets stems from their characteristic space-filling structure, which enables precise control over the structures and properties of surfaces and interfaces. It is expected that in the future, the development of materials for the realization of unique electronic states that reflect the two-dimensional nature and topology of assemblies will accelerate, leading to new functionalities. From various perspectives, triptycenes will continue to drive the development of functional materials that cannot be realized using planar molecules. Organic synthesis technologies will be the driving force to enable the precise design of such triptycene derivatives.

Acknowledgements This work was supported by JSPS KAKENHI (JP21H05024 and JP21H04690 for TF) and a Grant-in-Aid for Transformative Research Areas (A) "Condensed Conjugation" (JP20H05868 for TF). This work was also supported in part by the Research Program of "Five-Star Alliance" in "NJRC Mater. & Dev.".

Compliance with ethical standards

Conflict of interest The authors declare no competing interests.

Publisher's note Springer Nature remains neutral with regard to jurisdictional claims in published maps and institutional affiliations.

References

1. Chen C-F, Ma Y-X. Iptycenes chemistry, Springer Verlag: Berlin, Heidelberg; 2013.
2. Swager TM. Iptycenes in the design of high performance polymers. Acc Chem Res. 2008;41:1181–9.
3. Chong JH, MacLachlan MJ. Iptycenes in supramolecular and materials chemistry. Chem Soc Rev. 2009;38:3301–15.
4. Ma Y-X, Meng Z, Chen C-F. Synthesis of substituted iptycenes. Synlett 2015;26:6–30.
5. Zhao L, Li Z, Wirth T. Triptycene derivatives: synthesis and applications. Chem Lett. 2010;39:658–67.
6. Jiang Y, Chen C-F. Recent developments in synthesis and applications of triptycene and pentiptycene derivatives. Eur J Org Chem. 2011;2011:6377–403.
7. Khan N, Wirth T. Chiral triptycenes: concepts, progress and prospects. Chem A Eur J. 2021;27:7059–68.
8. Gu M-J, Wang Y-F, Han Y, Chen C-F. Recent advances on triptycene derivatives in supramolecular and materials chemistry. Org Biomol Chem. 2021;19:10047–67.
9. Wang Y, Ghanem BS, Ali Z, Hazazi K, Han Y, Pinnau I. Recent progress on polymers of intrinsic microporosity and thermally modified analogue materials for membrane-based fluid separations. Small Struct. 2021;2:2100049.
10. Woźny M, Mames A, Ratajczyk T. Triptycene derivatives: from their synthesis to their unique properties. Molecules. 2022;27:250.
11. Seiki N, Shoji Y, Kajitani T, Ishiwari F, Kosaka A, Hikima T, et al. Rational synthesis of organic thin films with exceptional long-range structural integrity. Science. 2015;348:1122–6.
12. Geng K, He T, Liu R, Dalapati S, Tan KT, Li Z, et al. Covalent organic frameworks: design, synthesis, and functions. Chem Rev. 2020;120:8814–933.
13. Klanderman BH, Faber JWH. Novel bridged anthracene derivatives and polyesters and copolyesters therefrom. J Polym Sci Part A Polym Chem. 1968;6:2955–65.

14. Hoffmeister E, Kropp JE, McDowell TL, Michel RH, Rippie WL. Triptycene polymers. J Polym Sci Part A Polym Chem. 1969;7:55–72.
15. Yang J-S, Swager TM. Fluorescent porous polymer films as TNT chemosensors: electronic and structural effects. J Am Chem Soc. 1998;120:11864–73.
16. Long TM, Swager TM. Molecular design of free volume as a route to low-κ dielectric materials. J Am Chem Soc 2003;125:14113–9.
17. Budd PM, Ghanem BS, Makhseed S, McKeown NB, Msayib KJ, Tattershall CE. Polymers of intrinsic microporosity (PIMs): robust, solution-processable, organic nanoporous materials. Chem Commun. 2004;40:230–1.
18. McKeown NB, Budd PM. Polymers of intrinsic microporosity (PIMs): organic materials for membrane separations, heterogeneous catalysis and hydrogen storage. Chem Soc Rev. 2006;35:675–83.
19. Low Z-X, Budd PM, McKeown NB, Patterson DA. Gas permeation properties, physical aging, and its mitigation in high free volume glassy polymers. Chem Rev. 2018;118:5871–911.
20. Côté AP, Benin AI, Ockwig NW, O'Keeffe M, Matzger AJ, Yaghi OM. Porous, crystalline, covalent organic frameworks. Science. 2005;310:1166–70.
21. Evans AM, Strauss MJ, Corcos AR, Hirani Z, Ji W, Hamachi LS, et al. Two-dimensional polymers and polymerizations. Chem Rev. 2021;122:442–564.
22. Payamyar P, King BT, Öttinger HC, Schlüter AD. Two-dimensional polymers: concepts and perspectives. Chem Commun. 2016;52:18–34.
23. Gong F, Mao H, Zhang Y, Zhang S, Xing W. Synthesis of highly sulfonated poly(arylene ether sulfone)s with sulfonated triptycene pendants for proton exchange membranes. Polymer. 2011;52:1738–47.
24. Kim Y, Moh LCH, Swager TM. Anion exchange membranes: enhancement by addition of unfunctionalized triptycene poly(-ether sulfone)s. ACS Appl Mater Interfaces. 2017;9:42409–14.
25. Terabe S, Konaka R. Electron spin resonance studies of bicyclo[2.2.1]heptanes and bicyclo[2.2.2]octanes spin labeled with nitrobenzene anion radicals. J Am Chem Soc. 1973;95:4976–86.
26. Zhang C, Chen C-F. Synthesis and structure of 2,6,14- and 2,7,14-trisubstituted triptycene derivatives. J Org Chem. 2006;71:6626–9.
27. Li P-F, Chen C-F. Synthesis, structures, and solid state self-assemblies of formyl and acetyl substituted triptycenes and their derivatives. J Org Chem. 2012;77:9250–9.
28. Chen Z, Swager TM. Synthesis and characterization of poly(2,6-triptycene). Macromolecules. 2008;41:6880–5.
29. Chakraborty S, Mondal S, Kumari R, Bhowmick S, Das P, Das N. Synthesis, characterization and DNA interaction studies of new triptycene derivatives. Beilstein J Org Chem. 2014;10:1290–8.
30. Mondala S, Das N. Triptycene based 1,2,3-triazole linked network polymers (TNPs): small gas storage and selective CO_2 capture. J Mater Chem A. 2015;3:23577–86.
31. Zhang Q-P, Wang Z, Zhang Z-W, Zhai T-L, Chen J-J, Ma H, et al. Triptycene-based chiral porous polyimides for enantioselective membrane separation. Angew Chem Int Ed. 2021;6:12781–5.
32. Ikai T, Yoshida T, Awata S, Wada Y, Maeda K, Mizuno M, et al. Circularly polarized luminescent triptycene-based polymers. ACS Macro Lett. 2018;7:364–9.
33. Alaslai N, Ma X, Ghanem B, Wang Y, Alghunaimi F, Pinnau I. Synthesis and characterization of a novel microporous dihydroxyl-functionalized triptycene-diamine-based polyimide for natural gas membrane separation. Macromol Rapid Commun. 2017;38:1700303.
34. Weidman JR, Luo S, Zhang Q, Guo R. Structure manipulation in triptycene-based polyimides through main chain geometry variation and its effect on gas transport properties. Ind Eng Chem Res. 2017;56:1868–79.
35. Park HB, Jung CH, Lee YM, Hill AJ, Pas SJ, Mudie ST, et al. Polymers with cavities tuned for fast selective transport of small molecules and ions. Science. 2007;318:254–8.
36. Yerzhankyzy A, Ghanem BS, Wang Y, Alaslai N, Pinnau I. Gas separation performance and mechanical properties of thermally-rearranged polybenzoxazoles derived from an intrinsically microporous dihydroxyl-functionalized triptycene diamine-based polyimide. J Membr Sci. 2020;595:117512.
37. Ji W, Li K, Shi W, Bai L, Li J, Ma X. The effect of chain rigidity and microporosity on the sub-ambient temperature gas separation properties of intrinsic microporous polyimides. J Membr Sci. 2021;635:119439.
38. Ye C, Luo C, Ji W, Weng Y, Li J, Yi S, et al. Significantly enhanced gas separation properties of microporous membranes by precisely tailoring their ultra-microporosity through bromination/debromination. Chem Eng J. 2023;451:138513.
39. Chong JH, MacLachlan MJ. Robust non-interpenetrating coordination frameworks from new shape-persistent building blocks. Inorg Chem. 2006;45:1442–4.
40. Mastalerz M, Sieste S, Cenić M, Oppel IM. Two-step synthesis of hexaammonium triptycene: an air-stable building block for condensation reactions to extended triptycene derivatives. J Org Chem. 2011;76:6389–93.
41. Hilton CL, Jamison CR, Zane HK, King BT. A triphenylene-based triptycene with large free volume synthesized by zirconium-mediated biphenylation. J Org Chem. 2009;74:405–7.
42. Duan Y, Zhang G, Liu X, Shi F, Wang T, Yan H, et al. Acene-extended triptycenes: synthesis, characterization, and singlet exciton fission properties. J Org Chem. 2022;87:8841–8.
43. Rabbani MG, Reich TE, Kassab RM, Jackson KT, El-Kaderi HM. High CO_2 uptake and selectivity by triptycene-derived benzimidazole-linked polymers. Chem Commun. 2012;48:1141–3.
44. Zhang X-M, Ding X, Hu A, Han B-H. Synthesis of Bergman cyclization-based porous organic polymers and their performances in gas storage. Polymer. 2017;118:249–55.
45. Bae S-Y, Kim D, Shin D, Mahmood J, Jeon I-Y, Jung S-M, et al. Forming a three-dimensional porous organic network via solid-state explosion of organic single crystals. Nat Commun 2017;8:1599.
46. Ghanem BS, Hashem M, Harris KDM, Msayib KJ, Xu M, Budd PM, et al. Triptycene-based polymers of intrinsic microporosity: organic materials that can be tailored for gas adsorption. Macromolecules. 2010;43:5287–94.
47. Peurifoy SR, Castro E, Liu F, Zhu X-Y, Ng F, Jockusch S, et al. Three-dimensional graphene nanostructures. J Am Chem Soc. 2018;140:9341–5.
48. Zhu Z, Swager TM. Conjugated polymers containing 2,3-dialkoxybenzene and iptycene building blocks. Org Lett. 2001;3:3471–4.
49. Williams VE, Swager TM. Iptycene-containing poly (aryleneethynylene)s. Macromolecules. 2000;33:4069–73.
50. Weidman JR, Luo S, Breier JM, Buckley P, Gao P, Guo R. Triptycene-based copolyimides with tailored backbone rigidity for enhanced gas transport. Polymer. 2017;126:314–23.
51. Zeng F, Tang L-L, Chen X-M, Ding M-H. Synthesis and physical properties of triptycene-based oligo(*p*-phenyleneethynylene)s. Tetrahedron. 2018;74:6917–21.
52. Gong F, Zhang S. Synthesis of poly(arylene ether sulfone)s with locally and densely sulfonated pentiptycene pendants as highly conductive polymer electrolyte membranes. J Power Sour. 2011;196:9876–83.

53. Long TM, Swager TM. Using "internal free volume" to increase chromophore alignment. J Am Chem Soc. 2002;124:3826–7.
54. Kim Y, Wang Y, France-Lanord A, Wang YMason, Wu Y-C, Lin S, et al. Ionic highways from covalent assembly in highly conducting and stable anion exchange membrane fuel cells. J Am Chem Soc. 2019;141:18152–9.
55. Corradoa TJ, Huanga Z, Huang D, Wamble N, Luo T, Guo R. Pentiptycene-based ladder polymers with configurational free volume for enhanced gas separation performance and physical aging resistance. Proc Natl Acad Sci USA 2021;118:e2022204118.
56. Vagin S, Ott A, Weiss H-C, Karbach A, Volkmer D, Rieger B. Metal-organic frameworks (MOFs) composed of (triptycenedicarboxylato)zinc. Eur J Inorg Chem. 2008;2008:2601–9.
57. VanVeller B, Robinson D, Swager TM. Triptycene diols: a strategy for synthesizing planar π systems through catalytic conversion of a poly(*p*-phenylene ethynylene) into a poly(*p*-phenylene vinylene). Angew Chem Int Ed. 2012;51:1182–6.
58. Sydlik SA, Delgado PA, Inomata S, VanVeller B, Yang Y, Swager TM, et al. Triptycene-containing polyetherolefins via acyclic diene metathesis polymerization. J Polym Sci Part A Polym Chem. 2013;51:1695–706.
59. Kuritani M, Sakata Y, Ogura F, Nakagawa M. Optically active triptycenes, V. Synthesis, optical resolution and absolute configuration of 2,7-disubstituted triptycenes. Bull Chem Soc Jpn. 1973;46:605–10.
60. Akutsu F, Inoki M, Kondo M, Inagawa T, Kayaki K, Kasashima Y. Synthesis and properties of novel polyarylates and poly(ether ether ketone)s derived from 2,7-triptycenediol. Polym J. 1997;29:1023–8.
61. Abdeljaber NO, Vinodh M, Al-Azemi TF. Host-guest properties of pagoda[4]arene with *α,ω*-dibromoalkanes and their self-assembled linear supramolecular polymer driven by guest halogen-halogen interactions. Tetrahedron. 2023;132:133240.
62. Quast H, Fuchsbauer H-L. ESR-spektroskopischer nachweis intramolekularer wechselwirkungen in radikalkationen von poly(α-methoxy)triptycenen. Chem Ber. 1986;119:1016–38.
63. Takemasa Y, Nozaki K. Synthesis of triptycenemonohydroquinonedibenzoquinone by comproportionation. J Org Chem. 2022;82:1502–6.
64. Matsumoto H, Nishimura Y, Arai T. Excited-state intermolecular proton transfer dependent on the substitution pattern of anthracene–diurea compounds involved in fluorescent ON^1–OFF–ON^2 response by the addition of acetate ions. Org Biomol Chem. 2017;15:6575–83.
65. Sydlik SA, Chen Z, Swager TM. Triptycene polyimides: soluble polymers with high thermal stability and low refractive indices. Macromolecules. 2011;44:976–80.
66. Rose I, Carta M, Malpass-Evans T, Ferrari M-C, Bernardo P, Clarizia G, et al. Highly permeable benzotriptycene-based polymer of intrinsic microporosity. ACS Macro Lett. 2015;4:912–5.
67. Swaidan R, Al-Saeedi M, Ghanem B, Litwiller E, Pinnau I. Rational design of intrinsically ultramicroporous polyimides containing bridgehead-substituted triptycene for highly selective and permeable gas separation membranes. Macromolecules. 2014;47:5104–14.
68. Zhang G, Presly O, White F, Oppel IM, Mastalerz M. A permanent mesoporous organic cage with an exceptionally high surface area. Angew Chem Int Ed. 2014;53:1516–20.
69. Rose I, Bezzu CG, Carta M, Comesana-Gandara B, Lasseuguette E, Ferrari MC, et al. Polymer ultrapermeability from the inefficient packing of 2D chains. Nat Mater. 2017;16:932–7.
70. Comesaña-Gándara B, Chen J, Bezzu CG, Carta M, Rose I, Ferrari M-C, et al. Energy Environ Sci. 2019;12:2733–40.
71. Ghanem B, Alghunaimi F, Ma X, Alaslai N, Pinnau I. Synthesis and characterization of novel triptycene dianhydrides and polyimides of intrinsic microporosity based on 3,3′-dimethylnaphthidine. Polymer. 2016;101:225–32.
72. Xiao Y-H, Shao Y, Ye X-X, Cui H, Wang D-L, Zhou X-H, et al. Microporous aromatic polyimides derived from triptycene-based dianhydride. Chin Chem Lett. 2016;27:454–8.
73. Rybáčková M, Bělohradský M, Holý P, Pohl R, Dekoj V, Závada J. Synthesis of highly symmetrical triptycene tetra- and hexacarboxylates. Synthesis. 2007;10:1554–8.
74. Ghanem BS, Alghunaimi F, Wang Y, Genduso G, Pinnau I. Synthesis of highly gas-permeable polyimides of intrinsic microporosity derived from 1,3,6,8-tetramethyl-2,7-diaminotriptycene. ACS Omega. 2018;3:11874–82.
75. Wang A, Tan R, Breakwell C, Wei X, Fan Z, Ye C, et al. Solution-processable redox-active polymers of intrinsic microporosity for electrochemical energy storage. J Am Chem Soc. 2022;144:17198–208.
76. Li Y, Cao R, Lippard SJ. Design and synthesis of a novel triptycene-based ligand for modeling carboxylate-bridged diiron enzyme active sites. Org Lett. 2011;13:5052–5.
77. Ishiwari F, Okabe G, Kajitani T, Fukushima T. Introduction of triptycene with a particular substitution pattern into polymer chains can dramatically improve the structural and rheological properties. ACS Macro Lett. 2021;10:1529–34.
78. Yu J, Itagaki A, Chen Y, Fukui T, Ishiwari F, Kajitani T, et al. Effective design for long-range polymer ordering using triptycene-containing side chains. Macromolecules. 2023;56:4556–65.
79. Ogiwara H, Ishiwari F, Kimura T, Yamashita Y, Kajitani T, Sugimoto A, et al. Changing the structural and physical properties of 3-arm star poly(*δ*-valerolactone)s by a branch-point design. Chem Commun. 2021;57:3901–4.
80. Ishiwari F, Okabe G, Ogiwara H, Kajitani T, Tokita M, Takata M, et al. Terminal functionalization with a triptycene motif that dramatically changes the structural and physical properties of an amorphous polymer. J Am Chem Soc. 2018;140:13497–502.
81. Chen Y, Ishiwari F, Fukui T, Kajitani T, Liu H, Liang X, et al. Overcoming the entropy of polymer chains by making a plane with terminal groups: a thermoplastic PDMS with a long-range 1D structural order. Chem Sci. 2023;14:2431–40.
82. Elbert SM, Rominger F, Mastalerz M. Synthesis of a rigid C_{3v}-symmetric tris-salicylaldehyde as a precursor for a highly porous molecular cube. Chem A Eur J. 2014;20:16707–20.
83. Elbert SM, Zhang W-S, Vaynzof Y, Oberhof N, Bernhardt M, Pernpointner M, et al. Metal-assisted salphen organic frameworks (MaSOFs) with trinuclear metal units for synergic gas sorption. Chem Mater. 2019;31:6210–23.
84. Leung FKC, Ishiwari F, Kajitani T, Shoji Y, Hikima T, Takata M, et al. Supramolecular scaffold for tailoring the two-dimensional assembly of functional molecular units into organic thin films. J Am Chem Soc. 2016;138:11727–33.
85. Gisbert Y, Abid S, Kammerer C, Rapenne G. Divergent synthesis of molecular winch prototypes. Chem A Eur J. 2021;27:16242–9.
86. Ishiwari F, Kawahara S, Kajitani T, Fukushima T. Structure-preserving solid-state thermal Huisgen cycloaddition polymerization of a self-assembled triptycene-based AB_3-type monomer. Chem Lett. 2021;50:2006–10.
87. Iwata T, Shindo M. Synthesis of 1,8,13-substituted triptycenes. Chem Lett. 2021;50:39–51.
88. Koo W-T, Kim Y, Savagatrup S, Yoon B, Jeon I, Choi S-J, et al. Porous ion exchange polymer matrix for ultrasmall Au nanoparticle-decorated carbon nanotube chemiresistors. Chem Mater. 2019;31:5413–20.

89. Koo W-T, Kim Y, Kim S, Suh BL, Savagatrup S, Kim J, et al. Hydrogen sensors from composites of ultra-small bimetallic nanoparticles and porous ion-exchange polymers. Chem. 2020;6:2746–58.
90. Luo SXL, Lin CJ, Ku KH, Yoshinaga K, Swager TM. Pentiptycene polymer/single-walled carbon nanotube complexes: applications in benzene, toluene, and *o*-xylene detection. ACS Nano. 2020;14:7297.
91. Concellón A, Castro-Esteban J, Swager TM. Ultratrace PFAS detection using amplifying fluorescent polymers. J Am Chem Soc. 2023;145:11420–30.
92. Guo S, Swager TM. Versatile porous poly(arylene ether)s *via* Pd-catalyzed C–O polycondensation. J Am Chem Soc. 2021;143:11828–35.
93. Liu RY, Guo S, Luo SXL, Swager TM. Solution-processable microporous polymer platform for heterogenization of diverse photoredox catalysts. Nat Commun. 2022;13:2775.
94. Carta M, Croad M, Malpass-Evans R, Jansen JC, Bernardo P, Clarizia G, et al. Triptycene induced enhancement of membrane gas selectivity for microporous Tröger's base polymers. Adv Mater. 2014;26:3526–31.
95. Wang Y-F, Li M, Teng J-M, Zhou H-Y, Zhao W-L, Chen C-F. Chiral TADF-active polymers for high-efficiency circularly polarized organic light-emitting diodes. Angew Chem Int Ed. 2021;60:23619–24.
96. Ikai T, Yoshida T, Shinohara K, Taniguchi T, Wada Y, Swager TM. Triptycene-based ladder polymers with one-handed helical geometry. J Am Chem Soc. 2019;141:4696–703.
97. Msayiba KJ, McKeown NB. Inexpensive polyphenylene network polymers with enhanced microporosity. J Mater Chem A. 2016;4:10110–3.
98. Amin MO, Al-Hetlani E, Antonangelo AR, Zhou H, Carta M. Ultrasonic-assisted removal of cationic and anionic dyes residues from wastewater using functionalized triptycene-based polymers of intrinsic microporosity (PIMs). Appl Water Sci. 2023;13:131.
99. Carta M, Croad M, Bugler K, Msayiba KJ, McKeown NB. Heterogeneous organocatalysts composed of microporous polymer networks assembled by Tröger's base formation. Polym Chem. 2014;5:5262–6.
100. Antonangelo AR, Hawkins N, Tocci E, Muzzi C, Fuoco A, Carta M. Tröger's base network polymers of intrinsic microporosity (TB-PIMs) with tunable pore size for heterogeneous catalysis. J Am Chem Soc. 2021;144:15581–94.
101. Kissel P, Murray DJ, Wulftange WJ, Catalano VJ, King BT. A nanoporous two-dimensional polymer by single-crystal-to-single-crystal photopolymerization. Nat Chem. 2014;6:774–8.
102. Bhola R, Payamyar P, Murray DJ, Kumar B, Teator AJ, Schmidt MU, et al. A two-dimensional polymer from the anthracene dimer and triptycene motifs. J Am Chem Soc. 2013;135:14134–41.
103. Grossmann L, King BT, Reichlmaier S, Hartmann N, Rosen J, Heck WM, et al. On-surface photopolymerization of two-dimensional polymers ordered on the mesoscale. Nat Chem. 2021;13:730–6.
104. Murray DJ, Patterson DD, Payamyar P, Bhola R, Song W, Lackinger M, et al. Large area synthesis of a nanoporous two-dimensional polymer at the air/water interface. J Am Chem Soc. 2015;137:3450–3.
105. Muller V, Hinaut A, Moradi M, Baljozovic M, Jung TA, Shahgaldian P, et al. A two-dimensional polymer synthesized at the air/water interface. Angew Chem Int Ed. 2018;57:10584–8.
106. Wang W, Shao F, Kröger M, Zenobi R, Schlüter AD. Structure elucidation of 2D polymer monolayers based on crystallization estimates derived from tip-enhanced Raman spectroscopy (TERS) polymerization conversion data. J Am Chem Soc. 2019;141:9867–71.
107. Shao F, Wang W, Yang W, Yang Z, Zhang Y, Lan J, et al. In-situ nanospectroscopic imaging of plasmon-induced two-dimensional [4+4]-cycloaddition polymerization on Au(111). Nat Commun. 2021;12:4557.
108. Norvez S. Liquid crystalline triptycene derivatives. J Org Chem. 1993;58:2414–8.
109. Hazell RG, Pawley GS, Lund Petersen CE. Crystal and molecular structure of triptycene, refined using constraint procedures. J Cryst Mol Struct. 1971;1:319–24.
110. Xu Q-M. Han M-J. Wan L-J. Wang C. Bai C-L. Dai B. et al. Tuning molecular orientation with STM at the solid/liquid interface. Chem Commun. 2003:2874–5. https://doi.org/10.1039/b308155a.
111. Imaizumi T, Takehara R, Yamashita Y, Yagi T, Ishiwari F, Shoji Y, et al. Thermal transport properties of an oriented thin film of a paraffinic tripodal triptycene. Jpn J Appl Phys. 2021;60:038002.
112. Matsutani A, Ishiwari F, Shoji Y, Kajitani T, Uehara T, Nakagawa M, et al. Chlorine-based inductively coupled plasma etching of GaAs wafer using tripodal paraffinic triptycene as an etching resist mask. Jpn J Appl Phys. 2016;55:06GL01.
113. Kumano M, Ide M, Seiki N, Shoji Y, Fukushima T, Saeki A. A ternary blend of a polymer, fullerene, and insulating self-assembling triptycene molecules for organic photovoltaics. J Mater Chem A. 2016;4:18490–8.
114. Yokota T, Kajitani T, Shidachi R, Tokuhara T, Kaltenbrunner M, Shoji Y, et al. A few-layer molecular film on polymer substrates to enhance the performance of organic devices. Nat Nanotechnol. 2018;13:139–44.
115. Kondo M, Kajitani T, Uemura T, Noda Y, Ishiwari F, Shoji Y, et al. Highly-ordered triptycene modifier layer based on blade coating for ultraflexible organic transistors. Sci Rep. 2019;9:9200.
116. Kondo M, Uemura T, Ishiwari F, Kajitani T, Shoji Y, Morita M, et al. Ultralow-noise organic transistors based on polymeric gate dielectrics with self-assembled modifiers. ACS Appl Mater Interfaces. 2019;11:41561–9.
117. Sugiyama M, Jancke S, Uemura T, Kondo M, Inoue Y, Namba N, et al. Mobility enhancement of DNTT and BTBT derivative organic thin-film transistors by triptycene molecule modification. Org Electron. 2021;96:106219.
118. Ishiwari F, Shoji Y, Fukushima T. Supramolecular scaffolds enabling the controlled assembly of functional molecular units. Chem Sci. 2018;9:2028–41.

Fumitaka Ishiwari received his B.E. and M.E. from Tokyo Institute of Technology, Japan in 2007 and 2008, respectively. He obtained his Ph.D. from Tokyo Institute of Technology in 2011, including a placement in the laboratory of Prof. Timothy M. Swager at Massachusetts Institute of Technology. In 2012, he started his academic carrier as an Assistant Professor at Chemical Resources Laboratory (currently, Laboratory for Chemistry and Life Science), Tokyo Institute of Technology. In 2020, he moved to Department of Applied Chemistry, Graduate School of Engineering, Osaka University as a Lecturer. His research interest includes supramolecular chemistry, self-assembly materials, chiral science and polymer science with a particular focus on ladder polymers.

Yoshiaki Shoji received his B.E. and M.E. from The University of Tokyo, Japan in 2003 and 2005, respectively. He was a JSPS Research Fellow from 2005 to 2008, receiving his Ph.D. in Engineering at The University of Tokyo in 2008. From 2008 to 2011, he worked as a RIKEN Research Fellow. During this period, he was a visiting researcher at the University of California, Riverside from 2010 to 2011. In 2011, he was appointed as an Assistant Professor at Chemical Resources Laboratory (currently, Laboratory for Chemistry and Life Science), Tokyo Institute of Technology, and was promoted to his current position in 2018. His research interest includes supramolecular chemistry and organoboron chemistry.

Colin John Martin obtained his B.A. in 2005 and Ph.D. in supramolecular chemistry, focusing on the analysis of polyaromatic hydrocarbons, in 2011 from Trinity College Dublin, Ireland. After spending four and a half years as a postdoctoral fellow in the group of Prof. Edwin Constable at Universitat Basel, Switzerland, he was appointed Assistant Professor at the NAIST-CEMES International Collaborative laboratory in both Nara, Japan, and Toulouse, France, in 2016. Then, in 2022, he moved to his current position as a Specially Appointed Assistant Professor at Laboratory for Chemistry and Life Science, Tokyo Institute of Technology. His current research interest includes self-assembling materials, with a particular focus on photo and electrochemical properties, and applications in charge transport and microscopy.

Takanori Fukushima received his B.S. and M.S. from Tohoku University, Japan in 1992 and 1994, respectively. He was a JSPS Research Fellow from 1995 to 1996 and received his Ph.D. in Science at Tohoku University in 1999. In 1996, he started his academic carrier as an Assistant Professor at the Department of Chemistry, Graduate School of Science, Tohoku University. In 2001, he moved to ERATO Aida Nanospace Project of Japan Science and Technology Agency (JST) as a researcher, and in 2004, he became a group leader of the same project. In 2007, he was appointed as a team leader at RIKEN Frontier Research System, which was reorganized as Advanced Science Institute in 2008. In 2010, he was appointed as Professor at Chemical Resources Laboratory (currently, Laboratory for Chemistry and Life Science), Tokyo Institute of Technology. In 2024, he became the Director of the Research Center for Autonomous Systems Materialogy (ASMat), Institute of Innovative Research, Tokyo Institute of Technology. His current research interest includes organic, physical organic, supramolecular and polymer chemistry, with a particular focus on molecular self-assemblies with π-electronic systems.